Groundwater Electro-Bioremediation via Diffuse Electro-Conductive Zones: A Critical Review

Journal Pre-proof

Groundwater Electro-Bioremediation via Diffuse Electro-Conductive Zones: A Critical Review

Federico Aulenta, Matteo Tucci, Carolina Cruz Viggi, Stefano Milia, Seyedmehdi Hosseini, Gianluigi Farru, Rajandrea Sethi, Carlo Bianco, Tiziana Tosco, Marios Ioannidis, Giulio Zanaroli, Riccardo Ruffo, Carlo Santoro, Ugo Marzocchi, Giorgio Cassiani, Luca Peruzzo

PII: S2666-4984(24)00130-3

DOI: https://doi.org/10.1016/j.ese.2024.100516

Reference: ESE 100516

To appear in: *Environmental Science and Ecotechnology*

Received Date: 18 July 2024

Revised Date: 21 November 2024

Accepted Date: 22 November 2024

Please cite this article as: F. Aulenta, M. Tucci, C. Cruz Viggi, S. Milia, S. Hosseini, G. Farru, R. Sethi, C. Bianco, T. Tosco, M. Ioannidis, G. Zanaroli, R. Ruffo, C. Santoro, U. Marzocchi, G. Cassiani, L. Peruzzo, Groundwater Electro-Bioremediation via Diffuse Electro-Conductive Zones: A Critical Review, *Environmental Science and Ecotechnology*, https://doi.org/10.1016/j.ese.2024.100516.

Diffuse electro-conductive zone (DECZ) for improved *in situ* electro-bioremediation

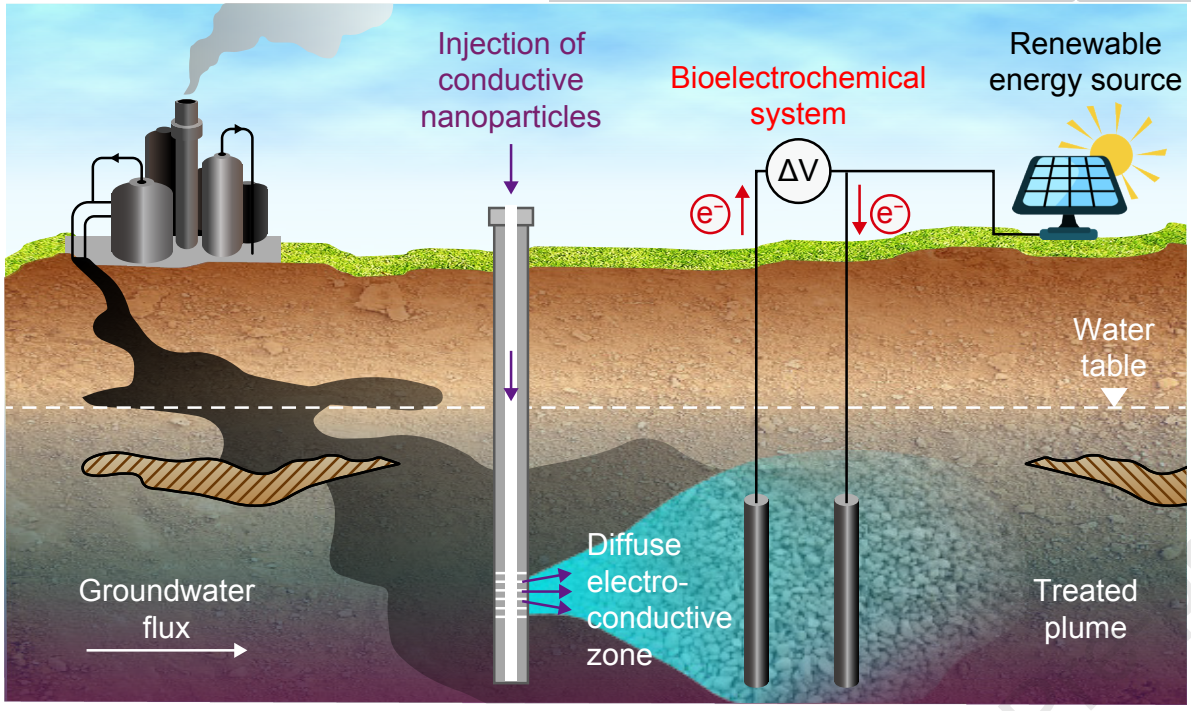

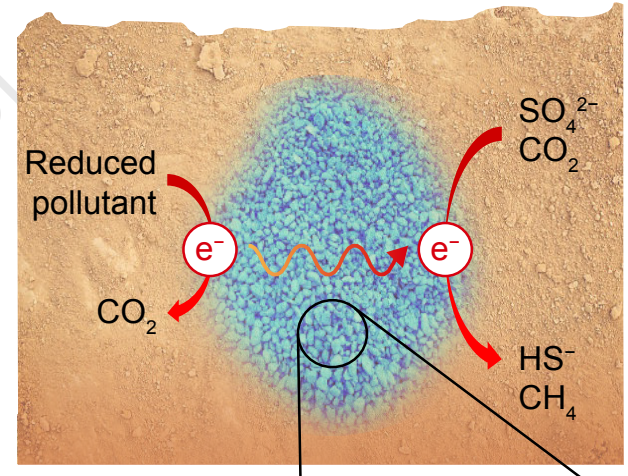

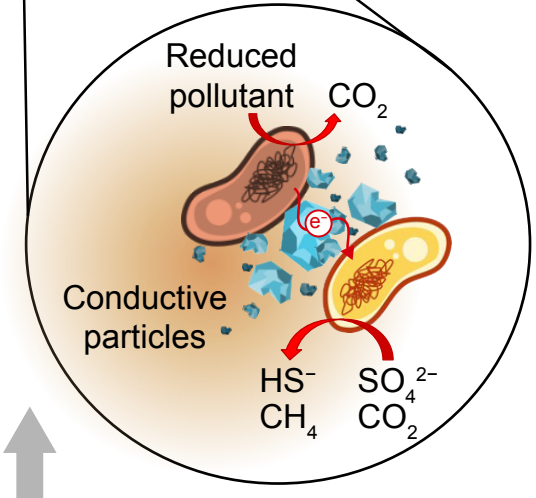

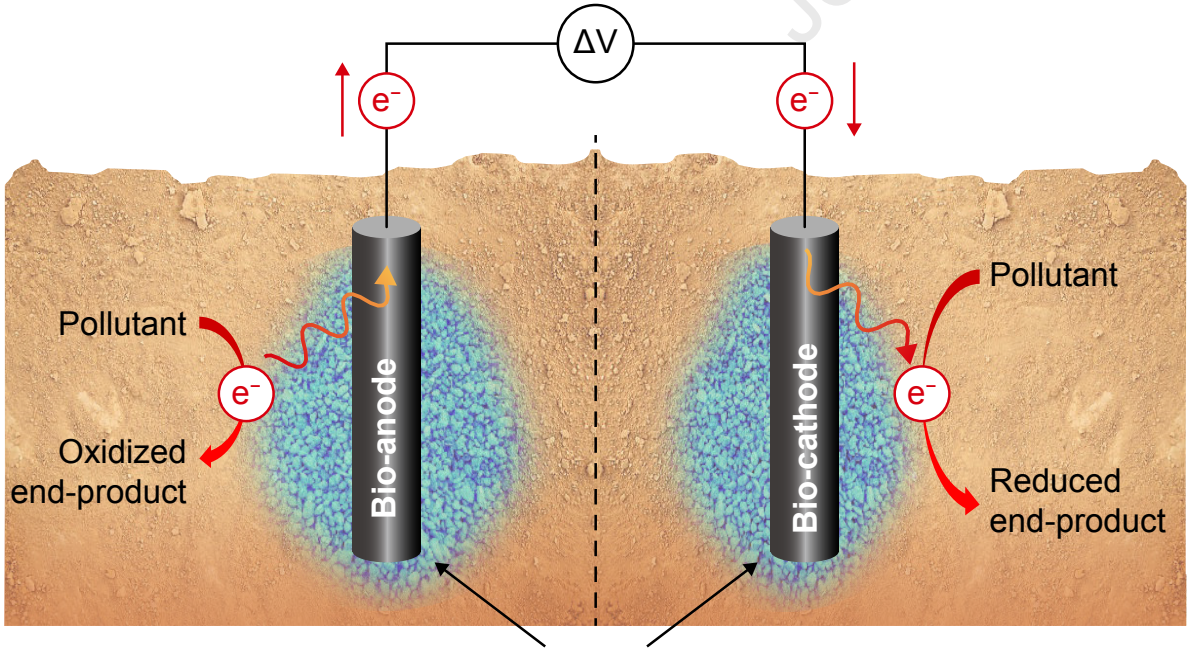

Diffuse electro-conductive zones

Groundwater Electro-Bioremediation via Diffuse Electro-Conductive Zones: A Critical Review

Federico Aulenta[a,*], Matteo Tucci[a], Carolina Cruz Viggi[a], Stefano Milia[b], Seyedmehdi Hosseini[c], Gianluigi Farru[c], Rajandrea Sethi[d], Carlo Bianco[d], Tiziana Tosco[d], Marios Ioannidis[d,e], Giulio Zanaroli[f], Riccardo Ruffo[g], Carlo Santoro[g], Ugo Marzocchi[h,i], Giorgio Cassiani[j], Luca Peruzzo[j]

[a] Water Research Institute (IRSA), National Research Council (CNR), Rome, Italy

[b] Institute for Environmental Geology and Geoengineering (IGAG), National Research Council (CNR), Cagliari, Italy

[c] Department of Civil, Environmental Engineering and Architecture, University of Cagliari, Cagliari, Italy

[d] Department of Environment, Land and Infrastructure Engineering & Clean Water Center, CWC, Politecnico di Torino, Torino, Italy

[e] Department of Chemical Engineering, University of Waterloo, Waterloo, Ontario, Canada

[f] Department of Civil, Chemical, Environmental and Materials Engineering, Alma Mater Studiorum University of Bologna, Bologna, Italy

[g] Department of Materials Science, University of Milano-Bicocca, Milano, Italy

[h] Department of Biology, Aarhus University, Aarhus, Denmark

[i] Center for Electromicrobiology, Aarhus University, Aarhus, Denmark

[j] Department of Geosciences, University of Padua, Padua, Italy

* Corresponding Author. E-mail: federico.aulenta@irsa.cnr.it; Tel: +39-0690672751; Fax: +39-0690672787; ORCID: 0000-0001-6819-7944

Abstract

Microbial electrochemical technologies (MET) can remove a variety of organic and inorganic pollutants from contaminated groundwater. However, despite significant laboratory-scale successes over the past decade, field-scale applications remain limited. We hypothesize that enhancing the electrochemical conductivity of the soil surrounding electrodes could be a groundbreaking and cost-effective alternative to deploying numerous high-surface-area electrodes in short distances. This could be achieved by injecting environmentally safe iron- or carbon-based conductive (nano)particles into the aquifer. Upon transport and deposition onto soil grains, these particles create an electrically conductive zone that can be exploited to control and fine-tune the delivery of electron donors or acceptors over large distances, thereby driving the process more efficiently. Beyond extending the radius of influence of electrodes, these diffuse electro-conductive zones (DECZ) could also promote the development of syntrophic anaerobic communities that degrade contaminants via direct interspecies electron transfer (DIET). In this review, we present the state-of-the-art in applying conductive materials for MET and DIET-based applications. We also provide a comprehensive overview of the physicochemical properties of candidate electrochemically conductive materials and related injection strategies suitable for field-scale implementation. Finally, we illustrate and critically discuss current and prospective electrochemical and geophysical methods for measuring soil electronic conductivity—both in the laboratory and in the field—before and after injection practices, which are crucial for determining the extent of DECZ. This review article provides critical information for a robust design and *in situ* implementation of groundwater electro-bioremediation processes.

1. Introduction

Anthropogenic pollution of groundwater by organic and inorganic contaminants (e.g., petroleum hydrocarbons, pharmaceuticals, brominated flame retardants, per- and poly-fluoroalkyl substances (PFAS), heavy metals, and nitrate) is an issue of ever-increasing relevance, particularly considering that more than half of the global freshwater supply for drinking, industrial uses, and irrigation comes from groundwater [1–5]. These contaminants' persistent threats to human, animal, and ecosystem health call for urgent remedies [6–8].

In the last decades, the expanding knowledge gathered on the ability of microorganisms to degrade or transform pollutants into harmless end-products and their degradative metabolic pathways has strikingly boosted the interest in bioremediation technologies for the cleanup of contaminated sites [9–11]. These are typically based on the possibility of manipulating environmental conditions by controlling the redox potential and/or by supplying nutrients, electron donors, or acceptors. However, the promise of bioremediation as a lower-cost, simpler, and more environmentally friendly alternative to conventional physical-chemical approaches is yet to be fully realized. Indeed, bioremediation is often associated with limited performance regarding process robustness and rates [12]. This is largely due to the limited availability of tools for domesticating the biological activity of the pollutant-degrading microbes in the contaminated matrix in time and space.

Approximately twenty years ago, research on microbial extracellular electron transfer started to gain significant traction [13,14]. The initial breakthrough technology was the microbial fuel cell, generating power from organic waste or sediments [15–17]. However, it soon became apparent that the influence of microbial electrochemical technologies (METs) extends far beyond this, impacting numerous other domains of industrial and environmental biotechnology, for example, allowing processes such as groundwater bioremediation to be driven by solid-state electron donors and acceptors in a highly flexible and controllable manner [18–22].

Unlike conventional bioremediation approaches that only provide one redox condition, METs can simultaneously reduce (at the cathode) and oxidize (at the anode) conditions. This process can even be integrated within a single treatment sequence, thus enabling the complete degradation (and detoxification) of contaminants with specific characteristics and complex mixtures [23–26]. The most noticeable feature of METs for *in situ* bioremediation is that the electrodes can be deployed within the contaminated matrix (i.e., soil, sediment, or groundwater). The electrodes can serve as virtually inexhaustible electron acceptors or donors for contaminants degradation (or removal via precipitation as in the case of metals), thus eliminating the need for the external, continual injection of

chemical amendments. Another key feature of MET is that the "energy level" of the electron donor/acceptor can be regulated, at least partially, using a power source, hence providing a unique tool for increasing, manipulating, and/or fine-tuning the rate and/or the selectivity of the target reaction(s) [19,20].

Furthermore, it is worth noting that since the electrode(s) may also support microbial growth, METs facilitate the co-localization of the electron donor/acceptor and the degrading microorganisms. Since many organic contaminants (e.g., petroleum hydrocarbons, emerging organic pollutants like pharmaceuticals) can be adsorbed on the surface of carbon-based electrodes, they tend to concentrate in a highly reactive zone where also the biocatalysts occur, and the electron donor/acceptor are simultaneously present [27].

Over the past few years, electro-bioremediation has attracted considerable interest in the scientific community, and several lab-scale studies have been published which have provided robust indications that MET can be employed for enhancing the biodegradation of a wide range of organic and inorganic soil and groundwater pollutants [19,28,29].

Despite this increasingly recognized potential, several hurdles still limit the transition of electro-bioremediation techniques from the laboratory to the field. The most striking is the lack of effective system configurations suitable for *in situ* applications. Indeed, being surface-based technologies, METs typically require high surface area electrodes to attain sufficiently high contaminants biodegradation rates and treat large, contaminated areas. In the case of large contamination plumes, this would ultimately result in unacceptably high costs of electrodes and consequent prohibitive capital expenditures (CAPEX) [28,30].

This review paper brings forward the intriguing hypothesis that making the surrounding of an electrode electrochemically conductive through the injection into the aquifer of low-cost and environmentally safe (metal- or carbon-based) conductive (nano)particles (Fig. 1a) could potentially represent a groundbreaking and cost-effective alternative to the use of multiple, high surface-area electrodes posted at a short distance one from each other. In other words, this approach would result in the creation within the aquifer of a so-called "diffuse electro-conductive zone (DECZ)," serving itself as a sink or source of electrons over high depths and long-distances and thus prompting the *in situ* bioremediation process more efficiently (Fig. 1b). Further to extending the radius-of-influence of electrodes, DECZ could also promote the development of syntrophic communities exploiting direct interspecies electron transfer process (DIET) [31–36] to anaerobically degrade organic contaminants under for instance, nitrate-reducing, sulfate-reducing, or methanogenic conditions (Fig. 1c) [37].

Figure 1.

In the past few years, some review papers dealing with the application of electro-bioremediation or DIET-based bioremediation approaches have been published in the scientific literature [19,20,38–45]. Most of these articles, however, have revolved around descriptions of the classes of treated contaminants, the involved (reductive or oxidative) biotransformation pathways, the key microorganisms, and related microbe-electrode extracellular electron transfer mechanisms, as well as the impact of key process parameters on treatment efficiency. To the best of our knowledge, none of these published documents has presented and discussed in a systematic manner practical strategies for *in situ* implementation of electro-bioremediation or DIET-based technologies.

In this specific context, the scope of the present review paper is to: (i) recall briefly fundamental aspects of cathodic, anodic, and DIET-based electro-bioremediation processes; (ii) identify key factors which presently limit treatment efficacy, with specific reference to the radius of influence (ROI) of electrodes; (iii) review strategies to create DECZ; (iv) review state-of-the-art methods to measure soil electronic conductivity at field- and laboratory-scale; (v) identify challenges and research needs for the future application of the DECZ concept in electro-bioremediation processes.

2. A brief overview of cathodic, anodic and DIET-based electro-bioremediation opportunities

2.1 Cathodic electro-bioremediation

The possibility of using (bio)cathodes in MET represents a promising and sustainable approach for groundwater remediation, as microbial processes occurring at the cathode (biocathode) can be exploited to facilitate the removal of several ubiquitous pollutants, including organic contaminants (e.g., chlorinated solvents), heavy metals, and nitrates, alone or in combination [46].

As for chlorinated organic compounds, their conversion into less chlorinated intermediates through reductive dechlorination (RD), carried out by organohalide-respiring bacteria (OHRB), is often limited by the slow metabolism of OHRB and the lack of sufficient external electron donors in groundwater [47]. In a recent study [48], direct electron transfer (DET) between *Axonexus* and *Desulfovibrio*/cathode and indirect electron transfer

(IET) via riboflavin for *Dehalococcoides* was shown to significantly enhance trichloroethene (TCE) dechlorination in MET biocathodes. A previous study [49] reported TCE sequential hydrogenolysis, with its main conversion into less harmful cis-1,2-dichloroethene and ethene as a minor product, in a two-chamber bioelectrochemical reactor (dechlorination efficiency was 99.1 ± 0.3%). Bio-cathodic TCE dechlorination to ethene in paddy soil was enhanced when a pure *D. mccartyi* NIT01 culture was added [50], and effective dechlorination was mainly attributed to microbial interactions through interspecies electron transfer. The possibility of simultaneously achieving reductive dechlorination of TCE and oxidation of toluene in a single-stage "bio-electrochemical well" simulating *in situ* treatment of multi-contaminated groundwater was also recently reported [23]. Toluene oxidation at the bioanode led to the current generation and hydrogen production at the cathode, which supported the reductive dechlorination of TCE to less-chlorinated intermediates and ethene. Results highlighted the potential for further optimization, especially concerning mass-transport limitations that might have constrained the system's efficiency. Zou et al. [51] investigated the removal of 2,4,6-trichlorophenol (TCP) at the biocathode of a two-chamber bioelectrochemical reactor treating constructed wetland (CW) sediments. Bioelectrochemical RD was inferred as the main metabolic mechanism in the closed-circuit experiments, with the cathode as the electron donor and acetate as the external carbon source for bacterial growth.

As reported previously [52], biocathodes may offer advantages for removing heavy metals such as chromium and vanadium, including no need for chemical additives and the use of bacteria for microbial catalysis. However, most of the studies focus on ex-situ applications, with *in situ* treatments requiring further exploration: Wu et al. [53] developed a Cr(VI)-reducing biocathode by reversing an anodic exoelectrogenic biofilm, achieving higher microbial density than traditional biocathodes; Beretta et al. [54]initially developed bio-anodes in a microbial fuel cell (MFC), then used them as cathodes in microbial electrolysis cell (MEC), observing high Cr(VI) removal efficiency (93%) at −0.300 V vs. SHE; Qiu et al. [55]exploited *Dysgonomonas* capability to reduce V(V) to V(IV) at the biocathode of an MFC at neutral pH, without the need for pH conditioning, achieving a power density output of 529±12 mW m^{-2}.

Among reducible inorganic contaminants, nitrate derived from agricultural-related activities is one of the most widespread pollutants [56]. As groundwater is usually characterised by low organic carbon concentration, autotrophic denitrification represents the key metabolism for successful nitrate removal using MET, where a solid-state, virtually inexhaustible electrode can provide the required electrons. Cecconet et al. [57] simulated

the *in situ* application of MET to achieve autotrophic denitrification. Ceballos-Escalera et al. [58] designed a compact tubular bioelectrochemical reactor suitable for decentralized applications in rural areas for simultaneous nitrate removal and groundwater disinfection. The system was capable of high nitrate removal rates (up to 5.0 ± 0.3 kg_{NO_3} m^{-3} d^{-1}), and *in situ* generation of free chlorine at the anode allowed effective water disinfection. In earlier studies, Puggioni and colleagues [56,59] treated saline groundwater with a novel three-chamber microbial MEC operated in galvanostatic mode (10 mA), achieving simultaneous autotrophic nitrate removal (bio-cathode), desalination (central compartment) and chlorine production (anode). Low specific energy consumption was observed ([6.8 ± 0.3]×10^{-2} kWh per gNO_3-$N_{removed}$), underpinning the system's efficiency while supporting three simultaneous processes.

2.2 Anodic electro-bioremediation

The microbially-catalyzed anodic oxidation of organic compounds in MET was initially used to reduce the chemical oxygen demand (COD) and biochemical oxygen demand (BOD) in domestic wastewater while simultaneously producing energy [60]. More recently, MET technologies were employed to stimulate the anaerobic oxidation of petroleum hydrocarbons [20]. In these systems, the anode collects electrons produced from the oxidation of organic contaminants. The anode electrode can be buried in anoxic benthic sediment or a contaminated aquifer and connected to a cathode in the overlying water. The anode can be pre-inoculated or naturally colonized by resident microbiota capable of electron transfer. Electrons from the anaerobic oxidation of contaminants flow through a connection to the cathode in the aerobic water column, where an oxygen reduction reaction (ORR) takes place. A similar setup can be used to stimulate bioremediation in hydrocarbon-contaminated aquifers. For example, a borehole anode can be an electron acceptor, with a cathode embedded several meters above the ground surface. A simpler configuration uses "electrochemical snorkels", which are conductive rods spanning aerobic and anaerobic zones, acting as both cathode and anode [61]. This configuration does not allow for power harvesting or activity monitoring.

Earlier studies reported using complex mixtures of highly contaminated refinery wastewater and diesel-contaminated groundwater as electron donors in MFCs [62,63], coupling hydrocarbon removal with power production. Diesel range organics (DRO) removal reached 82% when using an anode as an electron acceptor, compared to 31% in the open circuit control. Both alkanes and aromatic hydrocarbons were degraded in BES.

In recent studies, a novel reactor configuration called the "bioelectric well" was employed to treat synthetic groundwater containing single or multiple

contaminants [64,65]. Toluene is the easiest-to-degrade component among BTEX compounds (benzene, toluene, ethylbenzene, and xylenes), and its degradation was studied under various anode potentials using pure cultures and consortia [66]. Benzene was degraded in the anode of a BES by mixed cultures enriched from different environmental samples [67]. The degradation of polycyclic aromatic hydrocarbons (PAHs) was also reported in several studies. PAHs are persistent organic pollutants known for their carcinogenic, mutagenic, and teratogenic properties [68]. They are primarily found in soils (such as coal and tar deposits) and are produced by the thermal decomposition of organic matter. One study used sediment/soil-based MFCs to assess PAH degradation in polluted soils. The system enhanced anthracene, phenanthrene, and pyrene removal rates while generating electricity (12 mW m^{-2}) [69]. Although electricity production is a minor aspect of the technology, it serves as a valuable real-time indicator of degradation activity. Another study demonstrated the bioremediation capabilities of sediment MFCs in removing naphthalene, acenaphthene, and phenanthrene [70].

Interestingly, bioanodes have also successfully employed for the anaerobic oxidation of inorganic pollutants. As an example, Pous et al. [71] reported the oxidation of As(III) to As(V), a form which is more extensively and stably adsorbed onto metal-oxides, using a polarized graphite anode (+497 mV vs. SHE) serving as the terminal electron acceptor in the microbial metabolism.

2.3 DIET-based (electro)bioremediation

The discovery of DIET among microbial cells has brought attention to new and exciting strategies of microbial cooperation in energy-limited anaerobic ecosystems [72]. Specifically, when grown under selective conditions, *Geobacter metallireducens* and *Geobacter sulfurreducens* (two iron-reducing bacteria known for their ability to exchange electrons with extracellular, insoluble electron acceptors or donors) were found to form electro-conductive microbial aggregates. In these aggregates, electrons were transferred from *G. metallireducens* to *G. sulfurreducens* during the syntrophic degradation of ethanol, likely facilitated by *c*-type cytochromes.

This disruptive discovery challenged the established paradigm that electron exchange within mixed microbial communities occurs only through the diffusion of soluble molecules like H_2 or formate [73]. Experimental findings and theoretical calculations have pointed out that DIET is a significantly faster and more effective energy transfer mechanism than interspecies H_2 transfer [74]. This leads to the intriguing hypothesis that DIET may be more widespread in natural environments than previously recognized.

Interestingly, further studies reported that adding even small amounts of nano-sized magnetite nanoparticles (<50 mg Fe L^{-1}) could trigger DIET with

negligible lag-phase in syntrophic microbial communities and *Geobacter* species [75]. It was suggested that conductive magnetite particles attached to microbes served as abiotic electron conduits, in contrast to biological electron conduits like cytochromes, pilins, and pilin-like proteins, connecting redox reactions catalyzed by different microbial species [76]. More recently, a variety of conductive or semi-conductive minerals and materials such as pyrite, biochar, and graphite were found to substitute for biological connectors to promote and facilitate cell-to-cell DIET [77]

While DIET is now recognized as a key metabolic route in anaerobic digestion, its relevance in biogeochemistry and bioremediation remains largely unexplored despite a few significant publications highlighting its likely importance [39].

3. The radius of influence of electrodes in soils: a grand-challenge

As highlighted in the previous sections, microbiology is not likely the main limiting factor in developing *in situ* groundwater electro-bioremediation technologies. Indeed, under strictly controlled laboratory-scale conditions, electrochemical means were already successfully employed to enhance, steer, and control a broad (and ever-increasing) range of bioelectro-catalyzed reactions targeting a variety of oxidizable and reducing (organic and inorganic) groundwater contaminants.

In general, high-rate MET such as the MFC or the MEC, which aim to produce renewable energy from the oxidation of the organic matter contained in wastewater, suffer from the low conductivity of the electrolyte (i.e., the wastewater). In a landmark paper, Rozendal et al. [78] estimated electrolyte ohmic loss (i.e., the voltage loss caused by the movement of ions through the electrolyte) at the typical current densities and wastewater conductivities expected for bioelectrochemical wastewater treatment in practice. At a typical expected current density for full-scale systems of 10 A m^{-2}, referred to as the anode geometric area, the electrolyte ohmic loss encountered at such low conductivity would be ~1 V for each cm of distance between the anode and cathode. This makes the upscaling of MET for such applications extremely challenging. On the other hand, in other environmental applications such as groundwater remediation, the required rates of contaminants removal and the corresponding current densities can be orders of magnitude lower compared to those occurring in laboratory scale MFC or MEC, primarily due to the lower concentration levels of the contaminants which in most cases hardly exceed the ppm range (and more frequently fall within the ppb range) and the relatively low groundwater velocities. Thus, groundwater (ionic) conductivity is not expected to be a limiting factor for the field implementation of electro-bioremediation technologies. A recent

survey of literature [79] examined the impact of soil/groundwater conductivities on the electro-bioremediation of petroleum hydrocarbons. Interestingly, not only biodegradation occur in a broad range of electric conductivities, spanning from 0.2 mS cm^{-1} (i.e., non-saline soils) up to nearly 6 mS cm^{-1} (i.e., slightly saline soils), but also the process performance was only marginally affected by the electrolyte conductivity thus suggesting that this parameter alone cannot be a sufficient predictor of electro-bioremediation performance.

Conversely, the paper by Tucci and colleagues [79] identified the radius of influence (ROI) of soil-deployed electrodes as a main limiting factor of electro-bioremediation performance. Indeed, the effect of (bio)electrochemical stimulation was found to be confined within (maximum) 50 cm from the electrodes (Fig. 2). As an example, in a recent pilot-scale study employing a 50-L column-type bioelectrochemical system for the treatment of petroleum hydrocarbons, the removal efficiency was high (82–90%) in the proximity of the electrode (up to 35 cm) but rapidly declined at a further distance [80]. Based on a statistical assessment and some extrapolation, the authors hypothesized the ROI could be extended up to 90 cm by changing the design of the electrode. However, this speculation certainly warrants full-scale investigations.

Taken as a whole, this finding suggests that extending the ROI is an important consideration when large, contaminated groundwater plumes must be treated.

Figure 2.

One possible strategy to extend the ROI at a substantially greater distance could involve injecting conductive materials into the subsurface environment, provided that they can sustain long-distance electron transfer processes.

The impact of conductive materials on the performance of MET, in general, was well documented in the literature [77,81–83] though very few studies targeted specifically subsurface electro-bioremediation processes. Notably, most of these studies focused on adding carbon-based materials (e.g., biochar) to the soils to enhance electron transfer from microbes to electrodes [84–87]. One of these studies [87] reported a four-fold increase in the ROI of electrodes (from 4 to 16 cm) when biochar was mixed with the soil. A recent study [88] reported a method to create a conductive network within a soil matrix using magnetite nanoparticles to improve the interaction between microorganisms and hydrocarbons in a plant–rhizosphere bioelectrochemical system. This innovative approach accelerated the direct

interspecies electron transfer, leading to a 174–232% increase in contaminant removal (with a 24.1–29.2% removal rate) in the bioelectrochemical system with magnetite, compared to an 8.8% removal rate in the control bioelectrochemical system.

4. Fundamentals of electrical conductivity: electrons and/or ions "on the move."

4.1 Electronic vs. ionic soil conductivity

Electrical conductivity (EC), commonly expressed in S m^{-1}, is the ability of a material to conduct electric current. This is the reciprocal of the electrical resistivity (commonly expressed in Ω m), which instead represents the resistance a specific material offers to the passage of electrical current. Electrical conduction in solid matter (electronic conductivity) is conventionally triggered by the drift of free electrons in the solid. Electrical conductivity is a very important feature of solid materials. Solids can be distinguished into three types according to their electrical conductivity: conductors (or metals), insulators, and semiconductors. Interestingly, the latter category has intermediate conductivity compared to insulators and conductors. In metals, the conductivity decreases with the increase of the temperature. On the contrary, in semiconductors, the conductivity increases with temperature.

However, electrical conduction can also occur within liquids, where electricity is produced through the migration of ions (often referred to as ionic conductivity), positively or negatively charged, within the liquid. Indeed, by immersing two electrodes (positive and negative) in a liquid and applying an electromotive force (emf) across them, a current will flow through the liquid. When the electric field is created between the positive electrode (anode) and the negative electrode (cathode), ions flow through the liquid.

The positive ions drift in the direction of the current. Oppositely, the drift of negative ions is opposite the direction of the current. The electrical conductivity within a liquid strictly depends on the number of ions per unit of volume. It is also dependent on the drift velocity of the ions, and the latter depends mostly on (i) the intensity of the applied electric field and (ii) the electrical mobility of the ions, which in turn depends on the mass and the charge of the ion, and on the viscosity of the medium. Consequently, the electrical conductivity of different liquids is widely diverse depending on various variables.

For example, oily substances used as insulators in electrical systems possess very low conductivity (electrical resistivity values of 10^{-10} mΩ m). Water or alcohols considered pure solvents also have low electrical conductivity

quantified in 10^{-4} mΩ m (electrical resistivity). Adding chemical salts within pure water significantly reduces the electrical resistivity with values of 10 mΩ m. These are called electrolytic solutions and possess higher conductivity than pure solvents. For example, saturated sodium chloride solution has an electrical conductivity of ~20 m) m, much higher than the distilled water quantified in 2×10^{-4} mΩ m). However, it must be considered that the electrical conductivity of electrolytic solutions is way lower than the conductivity occurring, for example, in copper, which possesses conductivity values of 10^{8} mΩ m).

It is worth recalling that the electrical conductivity of a saturated porous medium is due to three distinct components: the conductivity attributable to the soil particles themselves (electronic conductivity), that of the pore water (ionic conductivity), and the surface conductivity. This latter can be regarded as an additional conductivity of an electrolyte in the proximity of a charged solid-liquid interface. Also, in this case, the conductivity is ensured by the drift of ionic species rather than electrons.

Given that most soil particles exhibit negligible bulk electronic conductivity due to their non-conductive material composition [89–91], the conductivity of the porous medium is predominantly determined by the contributions from pore water and surface conductivity [92–94]. Surface conductivity becomes particularly significant in soils rich in clay, as these materials feature an electrostatic double layer that plays a crucial role in electrical transport mechanisms [95,96]. Conversely, in coarse-grained soils, which are characterized by high hydraulic conductivity, low surface area, and limited clay content, the conduction process is primarily due to the ionic transport within the interconnected pore water, as described by Archie [97] and subsequently refined by successive models [98,99].

Overall, it is apparent that a noticeable difference exists between electronic conductivity, a physical property related to the ease of movement of electrons within solid materials, and ionic conductivity, which is more directly dependent on the ease of movement of ionic species in liquids. Importantly, while these two distinct properties are often interchangeably used or discussed in the scientific literature, especially when dealing with soils (wherein the solid, liquid and gas phases often coexist), they intrinsically refer to different phenomena. Notably, regarding the DECZ concept, the most critical conductivity to be considered is the electronic conductivity whereby electrons (rather than ions) are required to flow from an electrode to spatially distant electroactive microorganisms, or vice versa.

4.2 EC modification by subsurface injection of conductive materials

The injection of conductive micro or nanoparticles (CMNPs) directly into the groundwater system is envisioned as a possible strategy to enhance the

electronic conductivity of soils. In principle, this approach would potentially expand the radius of influence of bio-electrodes in optimal conditions but requires several concurrent factors to be carefully considered for its emplacement, including the type of CMNPs and related colloidal stability, injection regime, and approach, post-injection mobility, and costs.

Particles to enhance the electronic conductivity of natural porous media must exhibit high electrical conductivity and demonstrate suitable injectability into the subsurface, chemical stability over time, and environmental safety. The most promising CMNPs are metal- and carbon-based materials.

Several metals are characterized by high electrical conductivity (Table 1), exceeding values of 10^7 S m^{-1}. The conductivity in metals is fundamentally rooted in their electronic structure and the behaviour of electrons. Factors like lattice imperfections, impurities, and temperature can scatter electrons, reducing the mobility of electrons and conductivity. However, most metals used in electrochemistry are far too expensive (e.g., gold, platinum) or unsafe for remediation applications (e.g., silver, tin). Zerovalent iron (ZVI), which is commonly used in groundwater remediation applications [100], but also aluminum and, to a certain extent, copper, are instead characterized by both high electrical conductivity and reduced toxicity (Table 1). Nevertheless, under typical aquifer conditions, ZVI and aluminum particles, as well as most other metals, often undergo oxidation processes, forming an oxide layer on their surface. The bonding in metal oxides is predominantly ionic, where electrons are transferred from the metal to oxygen atoms, creating a lattice of positively and negatively charged metal ions. Therefore, incorporating oxygen into metal oxides significantly transforms the electronic structure of pure metals, drastically reducing their electrical conductivity, as detailed in (Table 1).

Alloys generally exhibit lower electrical conductivity than pure metals but still conduct electricity much better than metal oxides. This is because, unlike the ionic bonding in metal oxides, the metallic bonding in alloys still allows for electron mobility, albeit reduced.

Carbon-based materials exhibit various electrical conductivities, largely dependent on their specific structure and form [101]. For instance, graphite, a naturally occurring form of carbon, demonstrates high electrical conductivity due to its layered structure, allowing electrons to move freely along its planes. Conversely, diamond, another form of pure carbon, is an excellent electrical insulator under normal conditions because of its tightly bonded, tetrahedral lattice structure that restricts electron movement. The advent of synthetic carbon structures has significantly expanded the conductivity spectrum of carbon materials. Fullerenes, carbon nanotubes, and graphene are examples, with graphene being a standout for its exceptional electrical conductivity, reaching values as high as 10^8 S/m.

Graphene, a single layer of carbon atoms arranged in a hexagonal lattice, possesses remarkably high electron mobility at room temperature, making it one of the best conductors known. Carbon nanotubes, cylindrical molecules composed of rolled-up sheets of graphene, also exhibit extraordinary conductivity (ranging 10^4–10^7 S m^{-1}), which can be either metallic or semiconducting. A significant limitation of carbon nanotubes (CNTs) lies in their cytotoxicity and potential respiratory toxicity. However, ongoing research aims to address these challenges and unlock the full potential of CNTs across diverse applications. By functionalizing the surface of CNTs with biocompatible molecules, including polymers, peptides, and other biomolecules, their dispersibility can be enhanced, and the likelihood of adverse biological effects can be limited [102,103].

Other interesting carbon-based materials include carbon black, isotropic coke, and activated carbon, all holding comparable conductivities [104]. These unique properties make carbon-based materials highly versatile and promising CMNPs to be used for this specific purpose.

In soil EC enhancement applications, conductive materials must be injected into the subsurface to create a continuous, electrically conductive coating of the porous medium grains, thus improving the surface electronic conduction properties of the formation. Conductive materials have, therefore, to be much smaller than the size of the soil pores to optimally spread within the medium and cover the mineral grains sufficiently for a percolating path through electrically conductive material to exist without significantly reducing permeability. Therefore, Microscale and nanoscale conductive materials are preferred over larger particles that could lead to porous medium clogging and heterogeneous distribution within the aquifer. Conductive nanoparticles suitable for groundwater systems include metallic varieties such as zerovalent iron (NZVI) and carbon-based materials.

Choosing the optimal conductive material depends on several considerations, including site hydrogeological characteristics that may bind the injection method. Metal-based (nano)materials generally have substantially lower costs and higher availability than carbon-based materials [105]. Furthermore, it is worth mentioning that different iron-based (nano)materials are already commercially available and used for *in situ* groundwater remediation [106]. On the other hand, despite the increasing scientific interest due to key properties such as the eco-friendly nature, tunable microporosity and sorption properties [107], carbon-based (nano)materials are still limitedly employed for *in situ* groundwater remediation.

Regardless of the type of electrically conductive material, a major aspect that also needs to be considered is that when dimensions become very small, as in the case of nano-sized particles, the physical, chemical, biological, and

even toxicological properties of the material can become very different from those of the same material in bulk form. Hence, upon subsurface injection, it is necessary to understand the long-term fate and behaviour of such materials and verify whether, over time, they retain their pre-injection nominal size, structure, and related properties, including toxicity. Further research on these aspects is certainly warranted.

4.3 Colloidal stability of electrically conductive particles

Ensuring the colloidal stability of particles intended for injection is crucial for their effective distribution in the subsurface. The stability of these systems to sedimentation primarily depends on the particles' density and size, as described by Stokes' law. Similarly, their ability to avoid aggregation is influenced by the particles' nature, surface charge, and the chemistry of the water, among other factors, typically described through classical or extended Derjaguin-Landau-Verwey-Overbeek (DLVO) theory [108,109]. Carbon-based particles, characterized by small size distribution, low density, and high surface charge, exhibit a reduced tendency towards aggregation and sedimentation. Conversely, zero-valent iron particles, and more in general metal nanoparticles, are more susceptible to these processes due to their higher density and the magnetic interactions occurring among particles [110–112].

If the CMNPs are not stable enough, two primary approaches can be employed to mitigate particle aggregation and sedimentation: thermodynamic and kinetic stabilization. With thermodynamic stabilization, a suitable polymer is adsorbed on the surface of the particles to provide electrostatic, steric, or electrosteric stability. The stabilization effect is, therefore, due to electrostatic repulsion induced by the adsorbed polymer or by its physical presence in the case of the steric effect. Alternatively, kinetic stabilization can be achieved by dosing agents, increasing the viscosity and limiting the particles' Brownian motion. Prior research has indicated that biodegradable green polymers effectively provide steric and viscous (kinetic) stabilization for particle suspensions [113,114]. For instance, xanthan gum was an efficient medium for highly concentrated suspensions of NZVI and micrometric ZVI (MZVI), enhancing their permeability in column experiments and aiding the injection process [115,116]. This is attributed to the shear-thinning properties of the dispersions, where the viscosity of the fluid increases with a decrease in shear rate, which accompanies radial flow during injection. Consequently, biopolymer solutions improve the stability of iron dispersions during storage—owing to high viscosity that counteracts gravitational settling and particle aggregation—and facilitate injection procedures, which are performed at high shear rates, thereby reducing the fluid's viscosity.

4.4 Injection strategies

The field injection of CMNPs within the aquifer system can be implemented under two regimes (Fig. 3): permeation injection, which produces a uniform particle distribution in the subsurface, facilitating the contact between particles, contaminants, and bacteria [117]; and fracturing injection, which involves injecting fluids and particles at pressures exceeding the porous medium's critical fracturing pressure, potentially leading to higher migration distances, but also to an uneven distribution if not carefully managed [118].

Figure 3.

Permeation regime is often preferred due to the possibility of achieving more homogeneous particle distribution. However, this approach can be applied only in aquifer systems characterized by medium/high hydraulic conductivity and for injecting relatively small particles. To enhance the efficacy of material delivery through permeation, it is crucial to extend the ROI of the injection and minimize the injection pressure. Generally, larger ROIs, in the order of 1.5–2.5 m, have been reported at the field scale for the injection of fairly stable suspensions of micro- and nanoparticles dispersed in water-based solutions having viscosity close to water's, such as iron oxides [119–121]. Lower ROI, in the order of 0.7–1.5 m, has been reported for particles stabilized using viscous suspensions [113]. Reducing pressure during permeation injection is essential to prevent the generation of preferential flow paths [122] which would lead to inhomogeneous distribution of the CMNPs. Additionally, strategies must be implemented to prevent the accumulation of particles near the injection well, which could lead to the clogging of the porous medium and further increase pressure [123]. Achieving these objectives involves optimizing the properties of the particle suspension, particularly the colloidal stability and the operational conditions of the injection, tailored to the site-specific granulometry and permeability of the aquifer system [113]. As an example, the selection of the optimal injection discharge should meet two criteria: (i) it must be low enough to prevent exceeding the critical pressure of the porous medium that would generate preferential flow paths (and therefore deviating from the permeation regime), and (ii) yet high enough to maintain colloidal stability throughout the injection process. Thus, the optimal operating conditions are usually a compromise among maximizing the radius of influence, minimizing the injection time, and avoiding the risk of forming preferential paths. It's important to note that employing very low discharge rates and extending the

overall delivery time significantly increases costs due to prolonged field injection operations. Enhancing the delivery of particles and maximizing the ROI of permeation injections can also be achieved using CMNPs, which are stable from the colloidal point of view, e.g., by adding polymeric stabilizers. Principles similar to those discussed for the injection discharge also apply to determining the optimal stabilizer concentration to be dosed: it should be sufficiently high to keep the particles suspended for the duration of the injection yet low enough to avoid excessive pressure buildup in the well.

In groundwater remediation, permeation injections are often performed via ordinary wells or direct push systems operated at low pressures. In such conditions, the design of field-scale CMNP injections can be aided by transport models through a hybrid experimental-modelling approach. Specifically, an initial injection experiment in a radial transport setup provides data on the transport behaviours of a commercial NZVI-based reactive gel. Data analysis using the MNMs 2023 software [124] (https://areeweb.polito.it/ricerca/groundwater/software/mnms/) helps determine the kinetic parameters affecting NZVI particle movement in sandy porous media. These parameters then inform a comprehensive analysis that explores how changes in operational conditions and aquifer properties modify the injection's ROI. The findings facilitate the creation of diagrams that assist practitioners in designing particle suspensions and their injections for specific site conditions [113].

If the aquifer's formation is excessively tight or particle suspensions are unstable or overly coarse, permeation injection becomes impractical, necessitating fracturing injection to disperse CMNPs within the aquifer. This method involves maintaining a high injection rate to induce sufficient pressure in the well, exceeding the threshold for fracturing pressure and enabling preferential flow [118]. Repeating this process at consistent depth intervals makes a nearly uniform distribution of conductive particles around the injection point achievable, with ROI values potentially higher than permeation injection [118,125]. Hydrofracturing is typically executed via direct push techniques or valved tubing, as standard wells fail to offer controlled particle distribution, rendering them ineffective for this type of application.

4.5 Particle mobility and deposition

Upon injection, nanoparticles migrate and interact with the porous medium through a combination of hydrodynamic and physico-chemical mechanisms, which determine the final fate of the particles [126]. The physical deposition phenomena encompass mechanical dispersion, filtration, and straining, affecting individual particles and aggregates. Meanwhile, physico-chemical interactions between the particles and the porous medium induce dynamic

deposition and release phenomena, exhibiting variable behaviours during the initial and advanced deposition stages [127,128]. The colloidal deposition within porous media, under conditions of low particle concentration, can be effectively modelled and predicted by the clean bed filtration theory [129], whereas at higher particle concentrations, specialized numerical models such as Hydrus [130], MNMs, and MNM3D (developed at Politecnico di Torino) offer refined predictive capabilities [131,132]. While it is beneficial for CMNPs to migrate effectively during and immediately after injection to increase the ROI, ensuring high electrical conductivity requires proper contact between particles. In this regard, particles with limited mobility during injection, such as zerovalent iron, are less prone to remobilization afterwards, facilitating interparticle contact. Conversely, highly stable CMNPs like powdered carbon, iron oxides, and other metals are very mobile, which increases the risk of losing interparticle continuity. To address this, specific strategies can be applied to reduce particle mobility post-injection, thereby preventing losing connectivity and diminishing the effectiveness of the intervention [133].

4.6 Living conductive materials: the case of cable bacteria

Cable bacteria are multicellular, filamentous bacteria capable of conducting electrons over centimetre-long distances via periplasmatic fibres [134]. This allows them to couple oxygen or nitrate reduction at the sediment surface with sulfide oxidation at 2–3 cm [135–137]. This unique physiology appears to be restricted to specific members of the Desulfobulbacea family [138]. Species richness and morphological diversity within cable bacteria likely reflect their adaptation to various environmental conditions [139]. Accordingly, several studies indicate their ability to occupy diverse habitats, including marine, brackish, freshwater, and groundwater environments [140–144].

Their capacity to promote oxidation of sulfide to sulfate in anoxic sediment results in elevated rates of sulfate reduction [145], which in turn stimulates anaerobic degradation of organic pollutants such as alkanes, PAHs, pyrene, and toluene [146,147]. Besides contributing to the self-healing capacity of sediment and soil upon contamination, cable bacteria can potentially serve as self-regenerating conductive materials that could extend the radius of influence of subsurface-deployed electrodes. Although cable bacteria lack the genetic basis for "canonical" extracellular electron transport [148], they have been shown to electrically interface with electrodes [149].

In marine surface sediment, the co-presence of cable bacteria and bioelectrochemical snorkels resulted in alkane degradation rates equal to the sum of the two "components" alone, suggesting an additive effect [146]. Cable bacteria increased the thickness of the sulfide-free sediment horizon and reduced overall sulfide concentration compared to sediment with the

snorkel alone, confirming an extended volume of influence. pH microprofiles indicate that in the presence of the snorkel, cable bacteria grew over longer distances, possibly chasing the receding sulfidic horizon induced by bioelectrochemical sulfide oxidation on the snorkel surface. Persisting pH maxima at the sediment subsurface, compatible with cathodic oxygen reduction by cable bacteria [137], indicated that a significant portion of the cable bacteria population maintained contact with the oxygen diffusing from the overlying water and thereby did not extend from the electrode.

The detection of cable bacteria on the surface of anodes of MFC deployed in anoxic marine sediment supports the hypothesis that cable bacteria can use solid electron acceptors without oxygen [149]. In a recent study, Bonne and co-authors [150] inserted electrodes into a modified microscopy glass slide and provided visual evidence that cable bacteria enrich on an anode poised at +200 mV. Furthermore, inoculating cable bacteria in the slide increased the current generation fourfold compared to controls. However, this increase in current could be conclusively linked to cable bacteria due to other electroactive bacteria in the original inoculum. Overall, these observations support the hypothesis of a potential link between cable bacteria and electrodes in the absence of oxygen and nitrate, whereby cable bacteria connect to conductive material, radially expanding their volume of influence. The finding of aerobic bacteria closely associated with the anodic portion of the cable bacterial filaments led to the intriguing hypothesis of interspecies electron transfer, whereby aerobes can live in otherwise anoxic sediment by using cable bacteria as electron donors [151]. The same mechanisms were previously invoked to explain anomalous isotope labelling in sediment with cable bacteria [152]. If confirmed, such interactions may expand the repertoire of oxidative reactions induced by cable bacteria in anoxic sediment. Yet, limited experimental evidence on the occurrence and mechanisms regulating such interactions is available in the literature.

5. Measuring the electrical conductivity of soils: proving and sizing a DECZ

Measuring soil's electrical conductivity (and/or the electrical continuity) is not trivial due to the diverse and heterogeneous components of the matrix and the spatial variability of soil properties. One of the simplest methods is probably the electrical resistance method, preferably employed for analyzing (relatively small-sized) soil samples in the laboratory. Other electro-geophysical methods are more appropriate for field-scale noninvasive mapping and monitoring under saturated and unsaturated conditions. Although geophysical methods predominantly target ionic phenomena, they are also sensitive to the presence and continuity of electronic conductive

materials, traditionally consisting of ore particles and veins [153]. Therefore, they can be important for identifying and sizing DECZ.
The more commonly used electro-geophysical methods in this context are active: they are based on generating an electric field by applying a voltage difference between two current injection electrodes [154]. Among them, electric resistivity tomography (ERT) images have been explored more frequently to investigate the electric resistivity of the soil at the field scale, along with the induced polarization (IP) method, which extends the ERT method to measure polarization in addition to conductivity. In this paragraph, an overview of the cited methods is provided, and their potential applicability to the characterization of the DECZ is discussed.

5.1 Electrical resistance methods

The electrical resistance method is based on the application of the following fundamental equation: $R = L/(EC \times A)$, where EC is the electrical conductivity, L is the length of the sample, and A is the cross-sectional area of the piece of material to be investigated [155]. Resistance measurements involve the utilization of alternating currents (ACs) at extremely low frequencies (<30 Hz), thus avoiding capacitance and electrolytic effects and amplifier distortions [156]. A digital ohmmeter is then used to measure EC. This device is a probe composed of two metal electrodes. A constant current (I) is applied to the electrodes and the soil (sandwiched in the middle of the electrodes), and a voltage drop is measured across the two electrodes (ΔV). The soil resistance is calculated using Ohm's Law ($R = \Delta V/\mathrm{I}$). The EC can be calculated from the following equation: $EC = k\mathrm{I}/\Delta V$, where k is the ratio between length (l) and area (A), a known value for each probe.
The above-described basic electrical resistance (two-point) method suffers from the fact that the sensor measures not only the resistance of the conductor but also the resistance of the probe electrodes and the wiring. The four-point method overcomes such limitations. In the four-point method, two electrodes are used to inject the current into the soil, and two other electrodes are used for measuring the voltage drop. Thus, the electrode and wiring resistances are eliminated, and the interpretation of data is more straightforward. A schematic representation of the four-probe configuration is shown in Fig. 4 [157].

Figure 4.

As far as the electrical resistance methods are concerned, it should be noted again that current conduction (net charge movement) and polarization

(reversible charge separation) are fundamentally ionic processes in soils and rocks [158]. As previously explained, pore water dominates the current conduction under most conditions because the conductivity of the minerals is typically low. Hence, the conductivity strongly depends on the water saturation, salinity, and pore continuity [97]. Some minerals, most importantly clay, can contribute to the electrolytic conduction thanks to the adsorbed ions [159,160]. Hydrocarbons have low conductivity compared to typical pore waters [161]. Nonetheless, their spatial redistribution and alternation influence their impact on the conductivity of porous medium [162]. In fact, the arrangement of the individual elements within the porous medium (e.g., pore connectivity) significantly affects how their individual conductivities contribute to the overall "bulk" conductivity.

Electrolytic polarization arises when the movement of the ions is constrained by electrochemical interactions at the mineral-pore fluid interface [163]. Therefore, electrolytic polarization strongly relates to the extent and electrochemical properties of the mineral-pore fluid interfaces. As for conductivity, clays polarize more than other minerals thanks to their larger specific surface area and adsorption capacity [164]. Microbial cells and biofilms are a second source of electrolytic polarization due to their charged membranes, accumulating ions with limited mobility [165]. Electronic conduction in soils is typically limited to some oxides and sulfides of metals or regions with active redox reactions. In addition, a wide range of conductive particles have been increasingly used in environmental applications [35,166]. Electrolytic and electronic polarization are often distinguishable based on the polarization intensity, temporal scale, and prior information.

5.2 Application of Electrochemical Impedance Spectroscopy.

Although low-frequency AC is commonly used to determine soil EC, as discussed in the previous section, more information can be obtained by measuring the system's response over a wide range of frequencies (10^{-4}–10^{6} Hz). This method, which is widely used in electrochemistry, is called electrochemical impedance spectroscopy (EIS), and it is a powerful analytical technique used to investigate the electrical properties of materials, devices, and systems. EIS provides detailed insights into various processes such as charge transfer, diffusion, and double-layer capacitance and is widely used in studying batteries, fuel cells, corrosion, coatings, and sensors [167]. A key feature of EIS is its ability to deconvolute complex electrochemical phenomena into individual components, enabling precise analysis of system behaviours. Nyquist plots, a common way to represent EIS data, graphically display impedance with the real part on the x-axis and the imaginary part on the y-axis. These plots facilitate the identification of different impedance elements and the implementation of electrical circuit models, making it

easier to interpret and model the electrochemical processes occurring within the system.

Despite the technique's potential, there are few examples of using EIS in soil EC measurements. Following preliminary work highlighting the possibilities [168], EIS was applied to correlate soil EC with moisture content, showing soil impedance spectra (Nyquist plots) and constructing interpretative models in terms of equivalent circuits to deconvolve the different contributions [169]. Other recent examples of the application of EIS to soil analysis include determining the law of variation of electrical impedance of a saline sulphate soil under different salinity and water content conditions [170], describing the electrochemical properties and microstructure of silty soils with temperature changes [171], and obtaining a calibration function to derive water content in pyroclastic soils [172].

These works testify to EIS's possibilities in determining soil electrical properties; however, the increasingly frequent use of EIS is desirable in this field. Compared to traditional methods, EIS could not only provide a more accurate measurement of EC, with the selection of the appropriate frequency but also separate different contributions and allow the deconvolution of electronic conductivity, electrolytic conductivity and interfacial phenomena.

5.3 Electric resistivity tomography

Among electro-geophysical active methods, electric resistivity tomography (ERT) images the subsurface conductivity by measuring the distribution of the electric potential field resulting from the current injection with a set of potential electrodes. Field applications rely on tens of electrodes that are alternately used in pairs for current injection and measurement of the electric potential. Modern multi-channel resistivity meters enable fast and automatic acquisition of thousands of measurements. The measurements are chosen among the possible configurations according to the desired resolution, investigation depth, and spatial extension [173]. The positioning of the electrodes can also be adapted to control the spatial sensitivity of the ERT survey [174]. Electrodes are commonly and conveniently deployed on the surface, but borehole electrodes are advantageous when focusing on a specific volume at depth. Initial ERT breakthroughs came from the use of borehole electrodes for monitoring water tracers [175], solute-transport [176] and stimulated bioremediation [177,178]. Today, field applications range from the kilometre scale [179] to the sub-meter scale [180] and offer continuous monitoring over several months [181].

Several ERT investigations successfully characterized and monitored the distribution of organic compounds, their degradation, and the associated leachate and gas emissions. Caterina et al. [182] monitored the evolution of hydrocarbon contamination for two years using a surface array of electrodes.

They found that the microbial activity and seasonality controlled the spatiotemporal conductivity changes. Clément et al. [183] successfully monitored a leachate recirculation induced to stimulate anaerobic methanogenesis and biodegradation in a municipal waste landfill. Bichet et al. [184] also characterized the leachate infiltration below two landfills in the methanogenic phase. They concluded that ERT supported estimating the landfill thickness and concentration of organic materials and resulting leachate. Georgaki et al. [185] performed surface ERT surveys to improve landfill emissions estimation. André et al. [186] characterized the distribution of cellulose and lignin in a dry batch of anaerobic digestion (AD) before its inoculation. They found that the imaged regions of higher conductivity were associated with higher cellulose content (relative to the lignin regions) and higher methane production after the inoculation. Other examples of ERT studies on organic compounds include farm animal effluents [187], long-term monitoring of organic leachate from a landfill [188], olive oil mill waste [189], fuel spillage and remediation [190–192], tracking and extraction of light non-aqueous phase liquids (LNAPLs) [193–195], and mapping of dense non-aqueous phase liquids (DNAPLs) [196,197]. Atekwana and Atekwana [162] reviewed some additional applications to introduce the concept of biogeophysics. The above field observations are also well supported by laboratory studies. For example, Cassidy et al. [198] specifically investigated the conductivity changes associated with anaerobic, aerobic, and abiotic degradation of diesel fuel. The conductivity increases were significant in all three experiments but were greatest under anaerobic conditions, thanks to the organic acids that increased the electrolyte concentration and enhanced the mineral dissolution. Additionally, ERT has been widely used to define the hydrological setting in biogeochemical studies; see examples in Ref. [199,200].

5.4 Induced polarization method

The induced polarization (IP) method extends the ERT method to measure the polarization and the conductivity. IP can provide additional valuable information for MET and DIET, given the sensitivity of polarization to (i) electronically conductive particles, (ii) microbial cells, and (iii) geochemical changes associated with microbial activity. The polarization induced by the applied electric field is measured in the time or frequency domain [201,202]. In the time domain, measurements are performed by applying a direct current (DC) square wave voltage, similar to ERT. The DC voltage is applied for a few seconds to induce the medium's polarization and then temporally turned off to measure the polarization and its decay. In addition to the maximum value of polarization, polarization decay provides valuable information on the characteristic time of polarization (i.e., relaxation time).

In the frequency domain, a sequence of sinusoidal voltage waveforms is used instead, ranging from a few mHz to tens of kHz [163]. Measurements in the frequency domain are more time-consuming but directly capture the frequency dependence of the polarization [203].

Since its early description, IP sensitivity to dispersed electronic conductive particles has been fundamental in ore prospecting [204]. Most IP studies successfully approximated these particles as perfect capacitors. Electrons move toward the positive pole of the external field and accumulate at the boundary of the particle without charge transfer across the interface. Here, the coupling with the surrounding electrolyte is limited to forming an electrical double layer of counterions. The relaxation time is related to the radius of the particles [205] and the conductivity of the surrounding medium [206,207]. The intensity of the polarization is controlled by the volumetric content of conductive particles [204], their size [205], and their type [208]. In addition, particle surface insulation (passivation) can effectively hinder polarization [209]. Meanwhile, this insulation effect potentially limits the IP sensitivity to some ore deposits; it is rather promising for environmental applications that aim to monitor the condition of active surfaces.

Beyond the perfect-capacitor model, the relevance of the net redox charge transfer caused by the temporary accumulation of electrons and ions has also been studied [210–212]. Redox reactions allow some current to flow across the interface even at low frequency, reducing and delaying the interface's polarisation. Both reduction and delay (i.e., longer relaxation times) were theoretically described and experimentally confirmed, including the concentration of redox-active species [211] and particle anisotropy [213]. Personna et al. [214] monitored the increase in the IP response caused by iron sulfide mineralization during stimulated sulfate reduction. Interestingly, an IP increase preceded the formation of visible precipitate due to IP sensitivity to the incipient interfacial changes. Williams et al. [215] characterized the spatiotemporal evolution of stimulated microbial iron and sulfate reduction, taking advantage of the strong polarization signals. Flores-Orozco et al. [216] successfully imaged the injection pathways of zerovalent iron particles for groundwater remediation. The polarization increased by 20 % upon injection, with larger increases (50%) matching preferential flow and accumulation regions. Wu and Peruzzo [217] explored the effect of salinity and pH on the IP signals of micrometre-sized graphite in silica sand, varying the graphite concentration and particle size. In agreement with previous studies, the polarization initially increased when graphite was added up to around 10%. At higher concentrations, the increasing electrical interconnection among the particles hindered further polarization rises. Pore fluid conductivity and pH had minor but systematic effects over the explored graphite concentration range.

Atekwana and Slater [218] extensively reviewed IP use to detect microbial cells. Specifically, IP captures the low-frequency component of the dielectric effects that have long been observed in biological and medical experiments [219]. As for mineral interfaces, this low-frequency polarization arises from the ion diffusion processes near the membranes, known as α polarization [220,221]. More recently, Mellage et al. [222] performed laboratory column experiments to investigate the IP signature of anaerobic microbial processes in ferrihydrite-coated and pure silica sand. The polarization increased for low cell densities ($<10^8$ cells mL^{-1}) and then dominated the IP response, even relative to the electronic polarization of the iron coating. Importantly, the authors could successfully distinguish the polarization of microbial cells and silica sand based on their different polarization relaxation times. Zhang et al. [223] controlled laboratory tests to monitor the frequency-domain IP response to bacterial growth in suspension and silica sand. The polarization increased in both growing conditions and showed different relaxation times, attributed to the complexity of the interfacial polarization in the presence of bacterial protrusions. Aal et al. [224] obtained similar polarization increases while investigating the biodegradation of hydrocarbons in real soil samples. In line with the other studies, the authors attributed the enhanced polarization signals to the formation of biofilms imaged with scanning electron microscopy (SEM). Previous studies [225,226] investigated the polarization of plant tissues in frequency-domain IP, and both found very high values of polarization associated with the intra-cell (symplastic) current pathways. These studies are examples of how the IP method can successfully take advantage of the polarization of living cells, leveraging and extending the research done in bioelectrical impedance to new applications [227].

In addition to the intrinsic direct IP signature of microbial cells, the indirect effects of the associated biogeochemical changes have also been studied. Flores-Orozco et al. [216] studied the distribution of biogeochemical hotspots within an old municipal solid waste landfill. Based on successive excavation information, the authors found that the imaged regions of high polarization contained the highest amount of degradable organic carbons and evidence of biogeochemical degradation processes. On the contrary, the conductivity was most sensitive to leachate accumulation. A similar investigation was performed by Katona et al. [228], who imaged the distribution of anaerobic biogeochemical hotspots within a wetland in a low-altitude catchment. The IP surveys resolved the regions with the highest phosphate and organic acids concentrations, which were used as main proxies. AD depends on and potentially alters the pH conditions. Peruzzo et al. [229] found that even relatively small pH decreases (from 5.6 to 5.0) strongly reduced the polarization of silica sand by enhancing the interface protonation. The authors also showed that this pH effect remained dominant when changing

the pore fluid salinity over common soil values. These results agree with earlier investigations [163,230] which theoretically predicted and observed a minimum polarization at the silica isoelectric point (near pH 2). While these and other studies emphasized the sensitivity of IP to pH, the underlying mechanisms vary significantly, and the interpretation remains ambiguous in real soils, particularly if it is not supported by prior information. For example, previous studies [231,232] showed how pH-dependent or microbial-induced calcite precipitation increases the polarization response by modifying the surface morphology and electrochemical properties. Numerous other laboratory and field studies also highlighted the sensitivity to salinity [233,234] and hydrocarbons[235–237]. In conclusion, the IP method is sensitive to numerous phenomena naturally associated with DIET and MET. While promising, this sensitivity also calls for careful interpretations supported by multidisciplinary investigations and adequate prior information.

5.5 Mise-a-la-masse and MET Electrodes

The Mise-a-la-masse (MALM) method is less commonly used than ERT and IP, but it is considered the last electrical method here because of its specific potential for MET applications. MALM differs from ERT and IP in that it directly targets a specific conductive fluid or solid body, represented here by the MET electrodes with the possible surrounding conductive amendments. The key practical difference is that one of the two current electrodes is directly connected to the target. This way, its shape and conductivity are contrasted with the surrounding control. They can be inferred by the distribution of the electric field, which is mapped using a set of potential electrodes, like in ERT. The MALM method was traditionally developed to map ore bodies [238]. More recently, its use has been extended to environmental applications. A frequent application is the location of leaks and leachate pathways in landfills, owing to the formation of preferential current pathways [239]. For example, DeCarlo et al. [240] combined ERT and MALM results with numerical simulations to detect leachate accumulation below a high-density polyethylene liner of a large landfill (20–40 m deep). The MALM method has also been adapted to monitor the migration of injected tracers [241–243]. Perri et al. [244] extended these early works by adding the numerical simulation of the MALM response based on the resistivity model obtained with concurrent ERT surveys. The coupling of ERT and MALM can also provide further information on the regions where the current passes from the target body to the surroundings. These regions are commonly identified as current leaking regions; see Peruzzo et al. [245] and references therein. As for ERT and IP, the survey scale can vary from tens of meters [246] to laboratory centimetre scale [247]. Similarly, using borehole electrodes can significantly enhance the survey resolution [248]. While this possibility has yet to be

explored, the combination of ERT and MALM method appears to be a promising solution for mapping the effective radius of the MET electrodes in porous media.

5.6 Other geophysical methods and multidisciplinary approaches

This section focused on geophysical electrical methods due to their direct relevance for MET and DIET and wide use in related environmental applications. For completeness, it is appropriate to highlight the advantages of multidisciplinary investigations and, thus, possible contributions of other geophysical methods. For example, the frequency electromagnetic induction (FDEM) method is widely used to map the conductivity distribution over wide areas [249]. Instead of the ERT electrodes, an antenna containing a set of coils is more conveniently and quickly carried over the investigated area to induce and measure the current conduction in the subsurface. While the ERT imaging can better adapt to the required depth and lateral scales and resolutions, FDEM surveys are significantly faster. For this reason, the two methods are often used together: preliminary FDEM maps can guide the ERT surveys and then extend the ERT interpretations over the entire site. Ground penetrating radar (GPR) has characterised contaminated sites and remediation processes. Because GPR uses higher electromagnetic frequencies than FDEM, it is sensitive to the electrical permittivity of the subsurface, which is a valuable source of information in addition to the conductivity [162]. GPR antennas can also be used in boreholes, which is advantageous when monitoring specific regions at depth [250]. For example, early studies [193,251] combined surface and borehole ERT, FDEM, and GPR measurements to study contaminated sites. Similarly, seismic methods offer yet different and independent information; for example, they have been used to complement the characterization of waste deposits [252] or general hydrogeological conditions [253,254].

Modelling also offers an exceptional tool for understanding electrical conductivity in soils. However, no universal method exists to accurately represent conductivity in porous media [255]. One major limitation is the lack of comprehensive data on pore structures at multiple scales, which complicates the accuracy of models. As a result, models are often simplified based on pore size distribution. Research has shown that some low-porosity formations exhibit unexpectedly high conductivity compared to more porous rocks, highlighting the complexity of current flow in porous media. Additionally, electrical conductivity is influenced by pore volume and geometric properties such as pore interconnection and tortuosity. Further research is needed to improve the accuracy of the models to be a useful tool for environmental applications

6. Concluding remarks

Electro-bioremediation is increasingly recognized as a flexible and sustainable strategy to tackle the problem of groundwater contamination. A decisive milestone towards the market deployment of this technology will be the development of viable field implementation strategies. In this context, we have presented and critically analyzed the approach known as the "diffuse electro-conductive zone (DECZ)." This method, based on a review of contemporary advancements in the field, has the potential to address one of the most significant challenges associated with subsurface electro-bioremediation processes, namely, the small radius of influence of electrodes. Based on laboratory studies, carbon- and iron-based materials, with dimensions spanning from nanometer- to millimeter-scale, appear to be the most effective ones. However, filed applications remain extremely limited, and ad hoc protocols and methodologies for injection within the aquifers still need to be developed and validated. Analogously, the analytical protocols currently employed to measure soil electrical conductivity for agronomic practices appear inadequate to track the efficiency of injection or to size the extension of DECZ, as these protocols predominantly measure ionic conductivity instead of electronic conductivity. Electrochemical impedance spectroscopy holds some potential to overcome this problem since, at least in principle, it would allow discriminating among the two different types of conductivities. However, geophysical methods and techniques appear more appropriate and have a greater potential for field application.

CRediT author statement

Federico Aulenta: Conceptualization, Writing - Original Draft, Visualization, Project Administration, Funding Acquisition. **Stefano Milia**: Conceptualization, Visualization, Writing - Original Draft. **Seyedmehdi Hosseini**: Visualization, Writing - Original Draft. **Gianluigi Farru**: Visualization, Writing - Original Draft. **Carolina Cruz Viggi**: Visualization, Writing - Original Draft. **Matteo Tucci**: Visualization, Writing - Original Draft. **Rajandrea Sethi**: Conceptualization, Visualization, Writing - Original Draft, Project Administration, Funding Acquisition. **Carlo Bianco**: Visualization, Writing - Original Draft. **Tiziana Tosco**: Visualization, Writing - Original Draft. **Marios Ioannidis**: Visualization, Writing - Original Draft. **Giulio Zanaroli**: Conceptualization , Visualization, Writing - Original Draft, Project Administration, Funding Acquisition. **Riccardo Ruffo**: Visualization, Writing - Original Draft. **Carlo Santoro**: Visualization, Writing - Original Draft. **Ugo Marzocchi**: Visualization, Writing - Original Draft. **Giorgio**

Cassiani: Visualization, Writing - Original Draft. **Luca Peruzzo**: Visualization, Writing - Original Draft.

Declaration of competing interest

The authors declare that they have no known competing financial interests or personal relationships that could have appeared to influence the work reported in this paper.

Acknowledgements

We acknowledge financial support under the National Recovery and Resilience Plan (NRRP), Mission 4, Component 2, Investment 1.1, Call for tender No. 104 published on 2.2.2022 by the Italian Ministry of University and Research (MUR), funded by the European Union – NextGenerationEU– Project Title SteeRing GroundwatEr Electro-bioremediAtion with ConducTIVe ParticlEs (REACTIVE) – CUP: B53D23018110006 - Grant Assignment Decree No. 1048 adopted on July 14, 2023 by the Italian Ministry of University and Research (MUR).

References

1. Xie, M.; Zhang, X.; Jing, Y.; Du, X.; Zhang, Z.; Tan, C. Review on Research and Application of Enhanced In-Situ Bioremediation Agents for Organic Pollution Remediation in Groundwater. *Water (Switzerland)* **2024**, *16*, doi:10.3390/W16030456.
2. Mineo, S. Groundwater and Soil Contamination by LNAPL: State of the Art and Future Challenges. *Science of The Total Environment* **2023**, *874*, 162394, doi:10.1016/J.SCITOTENV.2023.162394.
3. Malik, A.; Katyal, D.; Narwal, N.; Kataria, N.; Ayyamperumal, R.; Khoo, K.S. Sources, Distribution, Associated Health Risks and Remedial Technologies for Inorganic Contamination in Groundwater: A Review in Specific Context of the State of Haryana, India. *Environ Res* **2023**, *236*, 116696, doi:10.1016/J.ENVRES.2023.116696.
4. Sadia, M.; Kunz, M.; ter Laak, T.; De Jonge, M.; Schriks, M.; van Wezel, A.P. Forever Legacies? Profiling Historical PFAS Contamination and Current Influence on Groundwater Used for Drinking Water. *Science of The Total Environment* **2023**, *890*, 164420, doi:10.1016/J.SCITOTENV.2023.164420.
5. Ravindiran, G.; Rajamanickam, S.; Sivarethinamohan, S.; Karupaiya Sathaiah, B.; Ravindran, G.; Muniasamy, S.K.; Hayder, G. A Review of the Status, Effects, Prevention, and Remediation of Groundwater Contamination for Sustainable Environment. *Water 2023, Vol. 15, Page 3662* **2023**, *15*, 3662, doi:10.3390/W15203662.
6. Sinha, D.; Prasad, P. Health Effects Inflicted by Chronic Low-Level Arsenic Contamination in Groundwater: A Global Public Health Challenge. *Journal of Applied Toxicology* **2020**, *40*, 87–131, doi:10.1002/JAT.3823.
7. Pradhan, B.; Chand, S.; Chand, S.; Rout, P.R.; Naik, S.K. Emerging Groundwater Contaminants: A Comprehensive Review on Their Health Hazards and Remediation Technologies. *Groundw Sustain Dev* **2023**, *20*, 100868, doi:10.1016/J.GSD.2022.100868.
8. Motlagh, A.M.; Yang, Z.; Saba, H. Groundwater Quality. *Water Environment Research* **2020**, *92*, 1649–1658, doi:10.1002/WER.1412.
9. Majone, M.; Verdini, R.; Aulenta, F.; Rossetti, S.; Tandoi, V.; Kalogerakis, N.; Agathos, S.; Puig, S.; Zanaroli, G.; Fava, F. In Situ Groundwater and Sediment Bioremediation: Barriers and Perspectives at European Contaminated Sites. *N Biotechnol* **2015**, *32*, 133–146, doi:10.1016/J.NBT.2014.02.011.
10. Kaur, G.; Kaur, G.; Krol, M.; Kaur Brar, S. Unraveling the Mystery of Subsurface Microorganisms in Bioremediation. *Curr Res Biotechnol* **2022**, *4*, 302–308, doi:10.1016/J.CRBIOT.2022.07.001.
11. Illman, W.A.; Alvarez, P.J. Performance Assessment of Bioremediation and Natural Attenuation. *Crit Rev Environ Sci Technol* **2009**, *39*, 209–270, doi:10.1080/10643380701413385.
12. Aulenta, F.; Pera, A.; Rossetti, S.; Petrangeli Papini, M.; Majone, M. Relevance of Side Reactions in Anaerobic Reductive Dechlorination Microcosms Amended with Different Electron Donors. *Water Res* **2007**, *41*, 27–38, doi:10.1016/J.WATRES.2006.09.019.
13. Bond, D.R.; Lovley, D.R. Electricity Production by Geobacter Sulfurreducens Attached to Electrodes. *Appl Environ Microbiol* **2003**, *69*, 1548–1555, doi:10.1128/AEM.69.3.1548-1555.2003/ASSET/F4A7F315-959D-4605-A43B-3B7D1386F8C7/ASSETS/GRAPHIC/AM0331568007.JPEG.

14. Rabaey, K.; Angenent, L.; Schröder, U.; Keller, J. Bioelectrochemical Systems: From Extracellular Electron Transfer to Biotechnological Application. *Water Intelligence Online* **2009**, *8*, doi:10.2166/9781780401621.
15. Logan, B.E.; Hamelers, B.; Rozendal, R.; Schröder, U.; Keller, J.; Freguia, S.; Aelterman, P.; Verstraete, W.; Rabaey, K. Microbial Fuel Cells: Methodology and Technology†. *Environ Sci Technol* **2006**, *40*, 5181–5192, doi:10.1021/ES0605016.
16. Logan, B.E. Exoelectrogenic Bacteria That Power Microbial Fuel Cells. *Nature Reviews Microbiology 2009 7:5* **2009**, *7*, 375–381, doi:10.1038/nrmicro2113.
17. Bond, D.R.; Holmes, D.E.; Tender, L.M.; Lovley, D.R. Electrode-Reducing Microorganisms That Harvest Energy from Marine Sediments. *Science (1979)* **2002**, *295*, 483–485, doi:10.1126/SCIENCE.1066771/SUPPL_FILE/1066771S2_THUMB.GIF.
18. Leitão, P.; Rossetti, S.; Nouws, H.P.A.; Danko, A.S.; Majone, M.; Aulenta, F. Bioelectrochemically-Assisted Reductive Dechlorination of 1,2-Dichloroethane by a Dehalococcoides-Enriched Microbial Culture. *Bioresour Technol* **2015**, *195*, 78–82, doi:10.1016/J.BIORTECH.2015.06.027.
19. Wang, X.; Aulenta, F.; Puig, S.; Esteve-Núñez, A.; He, Y.; Mu, Y.; Rabaey, K. Microbial Electrochemistry for Bioremediation. *Environmental Science and Ecotechnology* **2020**, *1*, 100013, doi:10.1016/J.ESE.2020.100013.
20. Daghio, M.; Aulenta, F.; Vaiopoulou, E.; Franzetti, A.; Arends, J.B.A.; Sherry, A.; Suárez-Suárez, A.; Head, I.M.; Bestetti, G.; Rabaey, K. Electrobioremediation of Oil Spills. *Water Res* **2017**, *114*, 351–370, doi:10.1016/J.WATRES.2017.02.030.
21. Aulenta, F.; Reale, P.; Canosa, A.; Rossetti, S.; Panero, S.; Majone, M. Characterization of an Electro-Active Biocathode Capable of Dechlorinating Trichloroethene and Cis-Dichloroethene to Ethene. *Biosens Bioelectron* **2010**, *25*, 1796–1802, doi:10.1016/J.BIOS.2009.12.033.
22. Feng, H.; Yang, W.; Zhang, Y.; Ding, Y.; Chen, L.; Kang, Y.; Huang, H.; Chen, R. Electroactive Microorganism-Assisted Remediation of Groundwater Contamination: Advances and Challenges. *Bioresour Technol* **2023**, *377*, 128916, doi:10.1016/J.BIORTECH.2023.128916.
23. Cruz Viggi, C.; Tucci, M.; Resitano, M.; Crognale, S.; Di Franca, M.L.; Rossetti, S.; Aulenta, F. Coupling of Bioelectrochemical Toluene Oxidation and Trichloroethene Reductive Dechlorination for Single-Stage Treatment of Groundwater Containing Multiple Contaminants. *Environmental Science and Ecotechnology* **2022**, *11*, 100171, doi:10.1016/J.ESE.2022.100171.
24. Tucci, M.; Carolina, C.V.; Resitano, M.; Matturro, B.; Crognale, S.; Pietrini, I.; Rossetti, S.; Harnisch, F.; Aulenta, F. Simultaneous Removal of Hydrocarbons and Sulfate from Groundwater Using a "Bioelectric Well." *Electrochim Acta* **2021**, *388*, 138636, doi:10.1016/j.electacta.2021.138636.
25. Resitano, M.; Tucci, M.; Mezzi, A.; Kaciulis, S.; Matturro, B.; D'Ugo, E.; Bertuccini, L.; Fazi, S.; Rossetti, S.; Aulenta, F.; et al. Anaerobic Treatment of Groundwater Co-Contaminated by Toluene and Copper in a Single Chamber Bioelectrochemical System. *Bioelectrochemistry* **2024**, *158*, 108711, doi:10.1016/J.BIOELECHEM.2024.108711.
26. Tucci, M.; Fernández-Verdejo, D.; Resitano, M.; Ciacia, P.; Guisasola, A.; Blánquez, P.; Marco-Urrea, E.; Cruz Viggi, C.; Matturro, B.; Crognale, S.; et al. Toluene-Driven Anaerobic Biodegradation of Chloroform in a Continuous-Flow Bioelectrochemical Reactor. *Chemosphere* **2023**, *338*, 139467, doi:10.1016/J.CHEMOSPHERE.2023.139467.
27. Zhang, T.; Gannon, S.M.; Nevin, K.P.; Franks, A.E.; Lovley, D.R. Stimulating the Anaerobic Degradation of Aromatic Hydrocarbons in Contaminated Sediments by Providing an

Electrode as the Electron Acceptor. *Environ Microbiol* **2010**, *12*, 1011–1020, doi:10.1111/J.1462-2920.2009.02145.X.

28. Saxena, G.; Thakur, I.S.; Kumar, V.; Shah, M.P. Electrobioremediation of Contaminants: Concepts, Mechanisms, Applications and Challenges. *Combined Application of Physico-Chemical and Microbiological Processes for Industrial Effluent Treatment Plant* **2020**, 291–313, doi:10.1007/978-981-15-0497-6_14/TABLES/2.
29. Li, W.W.; Yu, H.Q. Electro-Assisted Groundwater Bioremediation: Fundamentals, Challenges and Future Perspectives. *Bioresour Technol* **2015**, *196*, 677–684, doi:10.1016/J.BIORTECH.2015.07.074.
30. Puig, S.; Jourdin, L.; Kalathil, S. Editorial: Microbial Electrogenesis, Microbial Electrosynthesis, and Electro-Bioremediation. *Front Microbiol* **2021**, *12*, 742479, doi:10.3389/FMICB.2021.742479/BIBTEX.
31. Liu, F.; Rotaru, A.E.; Shrestha, P.M.; Malvankar, N.S.; Nevin, K.P.; Lovley, D.R. Magnetite Compensates for the Lack of a Pilin-Associated c-Type Cytochrome in Extracellular Electron Exchange. *Environ Microbiol* **2015**, *17*, 648–655, doi:10.1111/1462-2920.12485.
32. Chen, S.; Rotaru, A.E.; Shrestha, P.M.; Malvankar, N.S.; Liu, F.; Fan, W.; Nevin, K.P.; Lovley, D.R. Promoting Interspecies Electron Transfer with Biochar. *Scientific Reports 2014 4:1* **2014**, *4*, 1–7, doi:10.1038/srep05019.
33. Chen, S.; Rotaru, A.E.; Liu, F.; Philips, J.; Woodard, T.L.; Nevin, K.P.; Lovley, D.R. Carbon Cloth Stimulates Direct Interspecies Electron Transfer in Syntrophic Co-Cultures. *Bioresour Technol* **2014**, *173*, 82–86, doi:10.1016/J.BIORTECH.2014.09.009.
34. Liu, F.; Rotaru, A.E.; Shrestha, P.M.; Malvankar, N.S.; Nevin, K.P.; Lovley, D.R. Promoting Direct Interspecies Electron Transfer with Activated Carbon. *Energy Environ Sci* **2012**, *5*, 8982–8989, doi:10.1039/C2EE22459C.
35. Cruz Viggi, C.; Tucci, M.; Resitano, M.; Palushi, V.; Crognale, S.; Matturro, B.; Petrangeli Papini, M.; Rossetti, S.; Aulenta, F. Enhancing the Anaerobic Biodegradation of Petroleum Hydrocarbons in Soils with Electrically Conductive Materials. *Bioengineering* **2023**, *10*, 441, doi:10.3390/BIOENGINEERING10040441/S1.
36. Cruz Viggi, C.; Simonetti, S.; Palma, E.; Pagliaccia, P.; Braguglia, C.; Fazi, S.; Baronti, S.; Navarra, M.A.; Pettiti, I.; Koch, C.; et al. Enhancing Methane Production from Food Waste Fermentate Using Biochar: The Added Value of Electrochemical Testing in Pre-Selecting the Most Effective Type of Biochar. *Biotechnol Biofuels* **2017**, *10*, 1–13, doi:10.1186/S13068-017-0994-7/FIGURES/7.
37. Gieg, L.M.; Fowler, S.J.; Berdugo-Clavijo, C. Syntrophic Biodegradation of Hydrocarbon Contaminants. *Curr Opin Biotechnol* **2014**, *27*, 21–29, doi:10.1016/J.COPBIO.2013.09.002.
38. Tucci, M.; Cruz Viggi, C.; Esteve Núñez, A.; Schievano, A.; Rabaey, K.; Aulenta, F. Empowering Electroactive Microorganisms for Soil Remediation: Challenges in the Bioelectrochemical Removal of Petroleum Hydrocarbons. *Chemical Engineering Journal* **2021**, *419*, 130008, doi:10.1016/J.CEJ.2021.130008.
39. Aulenta, F.; Tucci, M.; Cruz Viggi, C.; Dolfing, J.; Head, I.M.; Rotaru, A.E. An Underappreciated DIET for Anaerobic Petroleum Hydrocarbon-Degrading Microbial Communities. *Microb Biotechnol* **2021**, *14*, 2–7, doi:10.1111/1751-7915.13654.
40. He, Y.; Zhou, Q.; Mo, F.; Li, T.; Liu, J. Bioelectrochemical Degradation of Petroleum Hydrocarbons: A Critical Review and Future Perspectives. *Environmental Pollution* **2022**, *306*, doi:10.1016/j.envpol.2022.119344.
41. Lan, J.; Wen, F.; Ren, Y.; Liu, G.; Jiang, Y.; Wang, Z.; Zhu, X. An Overview of Bioelectrokinetic and Bioelectrochemical Remediation of Petroleum-Contaminated Soils. *Environmental Science and Ecotechnology* **2023**, *16*, doi:10.1016/j.ese.2023.100278.

42. Rushimisha, I.E.; Li, X.; Han, T.; Chen, X.; Abdoul Magid, A.S.I.; Sun, Y.; Li, Y. Application of Biochar on Soil Bioelectrochemical Remediation: Behind Roles, Progress, and Potential. *Crit Rev Biotechnol* **2024**, *44*, 120–138, doi:10.1080/07388551.2022.2119547.
43. Wang, W.; Dong, J.; Zhao, H. In-Situ Remediation of Contaminated Groundwater by Bioelectrochemical System: A Review. *Int Biodeterior Biodegradation* **2025**, *196*, doi:10.1016/j.ibiod.2024.105914.
44. You, J.; Ji, Z.; Zhao, J.; Sun, H.; Ye, J.; Cheng, Z.; Kong, X.; Chen, J.; Chen, D. Configurations of Bioelectrochemical Reactor for Environmental Remediation: A Review. *Chemical Engineering Journal* **2023**, *471*, doi:10.1016/j.cej.2023.144325.
45. Zheng, L.; Cai, X.; Tang, J.; Qin, H.; Li, J. Bioelectrochemical Technologies for Soil and Sediment Remediation: Recent Advances and Future Perspectives. *J Environ Manage* **2024**, *370*, doi:10.1016/j.jenvman.2024.122602.
46. Ucar, D.; Zhang, Y.; Angelidaki, I. An Overview of Electron Acceptors in Microbial Fuel Cells. *Front Microbiol* **2017**, *8*, 248548, doi:10.3389/FMICB.2017.00643/BIBTEX.
47. Aulenta, F.; Majone, M.; Tandoi, V. Enhanced Anaerobic Bioremediation of Chlorinated Solvents: Environmental Factors Influencing Microbial Activity and Their Relevance under Field Conditions. *Journal of Chemical Technology & Biotechnology* **2006**, *81*, 1463–1474, doi:10.1002/JCTB.1567.
48. Chen, S.-H.; Li, Z.-T.; Zhao, H.-P. Bioelectrochemical System Accelerates Reductive Dechlorination through Extracellular Electron Transfer Networks. *Environ Res* **2023**, *235*, 116645, doi:10.1016/j.envres.2023.116645.
49. Chen, F.; Li, Z.-L.; Liang, B.; Yang, J.-Q.; Cheng, H.-Y.; Huang, C.; Nan, J.; Wang, A.-J. Electrostimulated Bio-Dechlorination of Trichloroethene by Potential Regulation: Kinetics, Microbial Community Structure and Function. *Chemical Engineering Journal* **2019**, *357*, 633–640, doi:10.1016/j.cej.2018.09.191.
50. Meng, L.; Yoshida, N.; Li, Z. Soil Microorganisms Facilitated the Electrode-Driven Trichloroethene Dechlorination to Ethene by Dehalococcoides Species in a Bioelectrochemical System. *Environ Res* **2022**, *209*, 112801, doi:10.1016/j.envres.2022.112801.
51. Zou, C.; Wang, M.; Chen, Y.; Qin, Y.; Zhao, Y.; Qiao, L.; Zhu, S.; Chen, T.; Yuan, Y. Effects of Different Cathodic Potentials on Performance, Microbial Community Structure and Function for Bioelectrochemical-Stimulated Dechlorination of 2,4,6-Trichlorophenol in Sediments. *Environ Res* **2023**, *216*, 114477, doi:10.1016/J.ENVRES.2022.114477.
52. Cecconet, D.; Callegari, A.; Capodaglio, A.G. Bioelectrochemical Systems for Removal of Selected Metals and Perchlorate from Groundwater: A Review. *Energies 2018, Vol. 11, Page 2643* **2018**, *11*, 2643, doi:10.3390/EN11102643.
53. Wu, X.; Zhu, X.; Song, T.; Zhang, L.; Jia, H.; Wei, P. Effect of Acclimatization on Hexavalent Chromium Reduction in a Biocathode Microbial Fuel Cell. *Bioresour Technol* **2015**, *180*, 185–191, doi:10.1016/J.BIORTECH.2014.12.105.
54. Beretta, G.; Daghio, M.; Tofalos, A.E.; Franzetti, A.; Mastorgio, A.F.; Saponaro, S.; Sezenna, E. Microbial Assisted Hexavalent Chromium Removal in Bioelectrochemical Systems. *Water 2020, Vol. 12, Page 466* **2020**, *12*, 466, doi:10.3390/W12020466.
55. Qiu, R.; Zhang, B.; Li, J.; Lv, Q.; Wang, S.; Gu, Q. Enhanced Vanadium (V) Reduction and Bioelectricity Generation in Microbial Fuel Cells with Biocathode. *J Power Sources* **2017**, *359*, 379–383, doi:10.1016/J.JPOWSOUR.2017.05.099.
56. Puggioni, G.; Milia, S.; Dessì, E.; Unali, V.; Pous, N.; Balaguer, M.D.; Puig, S.; Carucci, A. Combining Electro-Bioremediation of Nitrate in Saline Groundwater with Concomitant Chlorine Production. *Water Res* **2021**, *206*, 117736, doi:10.1016/J.WATRES.2021.117736.

57. Cecconet, D.; Bolognesi, S.; Callegari, A.; Capodaglio, A.G. Simulation Tests of in Situ Groundwater Denitrification with Aquifer-Buried Biocathodes. *Heliyon* **2019**, *5*, e02117, doi:10.1016/J.HELIYON.2019.E02117.
58. Ceballos-Escalera, A.; Pous, N.; Balaguer, M.D.; Puig, S. Nitrate Electro-Bioremediation and Water Disinfection for Rural Areas. *Chemosphere* **2024**, *352*, 141370, doi:10.1016/J.CHEMOSPHERE.2024.141370.
59. Puggioni, G.; Milia, S.; Unali, V.; Ardu, R.; Tamburini, E.; Balaguer, M.D.; Pous, N.; Carucci, A.; Puig, S. Effect of Hydraulic Retention Time on the Electro-Bioremediation of Nitrate in Saline Groundwater. *Science of The Total Environment* **2022**, *845*, 157236, doi:10.1016/J.SCITOTENV.2022.157236.
60. Logan, B.E.; Rabaey, K. Conversion of Wastes into Bioelectricity and Chemicals by Using Microbial Electrochemical Technologies. *Science (1979)* **2012**, *337*, 686–690, doi:10.1126/SCIENCE.1217412.
61. Viggi, C.C.; Presta, E.; Bellagamba, M.; Kaciulis, S.; Balijepalli, S.K.; Zanaroli, G.; Papini, M.P.; Rossetti, S.; Aulenta, F. The "Oil-Spill Snorkel": An Innovative Bioelectrochemical Approach to Accelerate Hydrocarbons Biodegradation in Marine Sediments. *Front Microbiol* **2015**, *6*, 152868, doi:10.3389/FMICB.2015.00881/BIBTEX.
62. Morris, J.M.; Jin, S. Feasibility of Using Microbial Fuel Cell Technology for Bioremediation of Hydrocarbons in Groundwater. *Journal of Environmental Science and Health, Part A* **2007**, *43*, 18–23, doi:10.1080/10934520701750389.
63. Morris, J.M.; Jin, S.; Crimi, B.; Pruden, A. Microbial Fuel Cell in Enhancing Anaerobic Biodegradation of Diesel. *Chemical Engineering Journal* **2009**, *146*, 161–167, doi:10.1016/J.CEJ.2008.05.028.
64. Palma, E.; Daghio, M.; Franzetti, A.; Petrangeli Papini, M.; Aulenta, F. The Bioelectric Well: A Novel Approach for in Situ Treatment of Hydrocarbon-Contaminated Groundwater. *Microb Biotechnol* **2018**, *11*, 112–118, doi:10.1111/1751-7915.12760.
65. Palma, E.; Espinoza Tofalos, A.; Daghio, M.; Franzetti, A.; Tsiota, P.; Cruz Viggi, C.; Papini, M.P.; Aulenta, F. Bioelectrochemical Treatment of Groundwater Containing BTEX in a Continuous-Flow System: Substrate Interactions, Microbial Community Analysis, and Impact of Sulfate as a Co-Contaminant. *N Biotechnol* **2019**, *53*, 41–48, doi:10.1016/J.NBT.2019.06.004.
66. Zhang, T.; Gannon, S.M.; Nevin, K.P.; Franks, A.E.; Lovley, D.R. Stimulating the Anaerobic Degradation of Aromatic Hydrocarbons in Contaminated Sediments by Providing an Electrode as the Electron Acceptor. *Environ Microbiol* **2010**, *12*, 1011–1020, doi:10.1111/J.1462-2920.2009.02145.X.
67. Rakoczy, J.; Feisthauer, S.; Wasmund, K.; Bombach, P.; Neu, T.R.; Vogt, C.; Richnow, H.H. Benzene and Sulfide Removal from Groundwater Treated in a Microbial Fuel Cell. *Biotechnol Bioeng* **2013**, *110*, 3104–3113, doi:10.1002/BIT.24979.
68. Patel, A.B.; Shaikh, S.; Jain, K.R.; Desai, C.; Madamwar, D. Polycyclic Aromatic Hydrocarbons: Sources, Toxicity, and Remediation Approaches. *Front Microbiol* **2020**, *11*, 562813, doi:10.3389/FMICB.2020.562813/BIBTEX.
69. Yu, B.; Tian, J.; Feng, L. Remediation of PAH Polluted Soils Using a Soil Microbial Fuel Cell: Influence of Electrode Interval and Role of Microbial Community. *J Hazard Mater* **2017**, *336*, 110–118, doi:10.1016/J.JHAZMAT.2017.04.066.
70. Sherafatmand, M.; Ng, H.Y. Using Sediment Microbial Fuel Cells (SMFCs) for Bioremediation of Polycyclic Aromatic Hydrocarbons (PAHs). *Bioresour Technol* **2015**, *195*, 122–130, doi:10.1016/J.BIORTECH.2015.06.002.

71. Pous, N.; Casentini, B.; Rossetti, S.; Fazi, S.; Puig, S.; Aulenta, F. Anaerobic Arsenite Oxidation with an Electrode Serving as the Sole Electron Acceptor: A Novel Approach to the Bioremediation of Arsenic-Polluted Groundwater. *J Hazard Mater* **2015**, *283*, 617–622, doi:10.1016/J.JHAZMAT.2014.10.014.
72. Summers, Z.M.; Fogarty, H.E.; Leang, C.; Franks, A.E.; Malvankar, N.S.; Lovley, D.R. Direct Exchange of Electrons within Aggregates of an Evolved Syntrophic Coculture of Anaerobic Bacteria. *Science (1979)* **2010**, *330*, 1413–1415, doi:10.1126/SCIENCE.1196526/SUPPL_FILE/SUMMERS.SOM.PDF.
73. Stams, A.J.M.; Plugge, C.M. Electron Transfer in Syntrophic Communities of Anaerobic Bacteria and Archaea. *Nature Reviews Microbiology 2009 7:8* **2009**, *7*, 568–577, doi:10.1038/nrmicro2166.
74. Cruz Viggi, C.; Rossetti, S.; Fazi, S.; Paiano, P.; Majone, M.; Aulenta, F. Magnetite Particles Triggering a Faster and More Robust Syntrophic Pathway of Methanogenic Propionate Degradation. *Environ Sci Technol* **2014**, *48*, 7536–7543, doi:10.1021/ES5016789/SUPPL_FILE/ES5016789_SI_001.PDF.
75. Kato, S.; Hashimoto, K.; Watanabe, K. Microbial Interspecies Electron Transfer via Electric Currents through Conductive Minerals. *Proc Natl Acad Sci U S A* **2012**, *109*, 10042–10046, doi:10.1073/PNAS.1117592109/SUPPL_FILE/PNAS.201117592SI.PDF.
76. Liu, F.; Rotaru, A.E.; Shrestha, P.M.; Malvankar, N.S.; Nevin, K.P.; Lovley, D.R. Magnetite Compensates for the Lack of a Pilin-Associated c-Type Cytochrome in Extracellular Electron Exchange. *Environ Microbiol* **2015**, *17*, 648–655, doi:10.1111/1462-2920.12485.
77. Cheng, Q.; Call, D.F. Hardwiring Microbes via Direct Interspecies Electron Transfer: Mechanisms and Applications. *Environ Sci Process Impacts* **2016**, *18*, 968–980, doi:10.1039/C6EM00219F.
78. Rozendal, R.A.; Hamelers, H.V.M.; Rabaey, K.; Keller, J.; Buisman, C.J.N. Towards Practical Implementation of Bioelectrochemical Wastewater Treatment. *Trends Biotechnol* **2008**, *26*, 450–459, doi:10.1016/J.TIBTECH.2008.04.008.
79. Tucci, M.; Cruz Viggi, C.; Esteve Núñez, A.; Schievano, A.; Rabaey, K.; Aulenta, F. Empowering Electroactive Microorganisms for Soil Remediation: Challenges in the Bioelectrochemical Removal of Petroleum Hydrocarbons. *Chemical Engineering Journal* **2021**, *419*, 130008, doi:10.1016/j.cej.2021.130008.
80. Akbari, A.; Ghoshal, S. Pilot-Scale Bioremediation of a Petroleum Hydrocarbon-Contaminated Clayey Soil from a Sub-Arctic Site. *J Hazard Mater* **2014**, *280*, 595–602, doi:10.1016/J.JHAZMAT.2014.08.016.
81. Gacitúa, M.A.; González, B.; Majone, M.; Aulenta, F. Boosting the Electrocatalytic Activity of Desulfovibrio Paquesii Biocathodes with Magnetite Nanoparticles. *Int J Hydrogen Energy* **2014**, *39*, 14540–14545, doi:10.1016/J.IJHYDENE.2014.07.057.
82. Cruz Viggi, C.; Casale, S.; Chouchane, H.; Askri, R.; Fazi, S.; Cherif, A.; Zeppilli, M.; Aulenta, F. Magnetite Nanoparticles Enhance the Bioelectrochemical Treatment of Municipal Sewage by Facilitating the Syntrophic Oxidation of Volatile Fatty Acids. *Journal of Chemical Technology & Biotechnology* **2019**, *94*, 3134–3146, doi:10.1002/JCTB.6120.
83. Viggi, C.C.; Colantoni, S.; Falzetti, F.; Bacaloni, A.; Montecchio, D.; Aulenta, F. Conductive Magnetite Nanoparticles Enhance the Microbial Electrosynthesis of Acetate from CO2 While Diverting Electrons Away from Methanogenesis. *Fuel Cells* **2020**, *20*, 98–106, doi:10.1002/FUCE.201900152.
84. Li, X.; Li, Y.; Zhang, X.; Zhao, X.; Sun, Y.; Weng, L.; Li, Y. Long-Term Effect of Biochar Amendment on the Biodegradation of Petroleum Hydrocarbons in Soil Microbial Fuel Cells.

Science of The Total Environment **2019**, *651*, 796–806, doi:10.1016/J.SCITOTENV.2018.09.098.

85. Li, X.; Wang, X.; Zhao, Q.; Wan, L.; Li, Y.; Zhou, Q. Carbon Fiber Enhanced Bioelectricity Generation in Soil Microbial Fuel Cells. *Biosens Bioelectron* **2016**, *85*, 135–141, doi:10.1016/J.BIOS.2016.05.001.
86. Li, X.; Wang, X.; Zhang, Y.; Zhao, Q.; Yu, B.; Li, Y.; Zhou, Q. Salinity and Conductivity Amendment of Soil Enhanced the Bioelectrochemical Degradation of Petroleum Hydrocarbons OPEN. *Nature Publishing Group* **2016**, doi:10.1038/srep32861.
87. Cai, X.; Yuan, Y.; Yu, L.; Zhang, B.; Li, J.; Liu, T.; Yu, Z.; Zhou, S. Biochar Enhances Bioelectrochemical Remediation of Pentachlorophenol-Contaminated Soils via Long-Distance Electron Transfer. *J Hazard Mater* **2020**, *391*, 122213, doi:10.1016/J.JHAZMAT.2020.122213.
88. Zhang, X.; Li, R.; Wang, J.; Liao, C.; Zhou, L.; An, J.; Li, T.; Wang, X.; Zhou, Q. Construction of Conductive Network Using Magnetite to Enhance Microflora Interaction and Petroleum Hydrocarbons Removal in Plant-Rhizosphere Microbial Electrochemical System. *Chemical Engineering Journal* **2022**, *433*, 133600, doi:10.1016/J.CEJ.2021.133600.
89. Zainal Abidin, M.H.; Ahmad, F.; Chitral Wijeyesekera, D.; Saad, R.; Baharuddin, M.F.T. Soil Resistivity Measurements to Predict Moisture Content and Density in Loose and Dense Soil. *Applied Mechanics and Materials* **2013**, *353–356*, 911–917, doi:10.4028/WWW.SCIENTIFIC.NET/AMM.353-356.911.
90. Soares Gerscovich, D.M.; Vipulanandan, C. Data Analyses to Correlate the Soil Properties to the Electrical Resistivity. *Geotechnical and Geological Engineering* **2023**, *41*, 4507–4528, doi:10.1007/S10706-023-02529-Y/METRICS.
91. Deiana, R.; Cassiani, G.; Villa, A.; Bagliani, A.; Bruno, V. Calibration of a Vadose Zone Model Using Water Injection Monitored by GPR and Electrical Resistance Tomography. *Vadose Zone Journal* **2008**, *7*, 215–226, doi:10.2136/VZJ2006.0137.
92. Godio, A.; Naldi, M. Two-Dimensional Electrical Imaging for Detection of Hydrocarbon Contaminants. *Near Surface Geophysics* **2003**, *1*, 131–137, doi:10.3997/1873-0604.2003003.
93. Koroma, S.; Arato, A.; Godio, A. Analyzing Geophysical Signature of a Hydrocarbon-Contaminated Soil Using Geoelectrical Surveys. *Environ Earth Sci* **2015**, *74*, 2937–2948, doi:10.1007/S12665-015-4326-6/FIGURES/9.
94. Slater, L.; Binley, A.; Versteeg, R.; Cassiani, G.; Birken, R.; Sandberg, S. A 3D ERT Study of Solute Transport in a Large Experimental Tank. *J Appl Geophy* **2002**, *49*, 211–229, doi:10.1016/S0926-9851(02)00124-6.
95. Revil, A. Effective Conductivity and Permittivity of Unsaturated Porous Materials in the Frequency Range 1 MHz–1GHz. *Water Resour Res* **2013**, *49*, 306–327, doi:10.1029/2012WR012700.
96. Revil, A.; Cathles, L.M.; Losh, S.; Nunn, J.A. Electrical Conductivity in Shaly Sands with Geophysical Applications. *J Geophys Res Solid Earth* **1998**, *103*, 23925–23936, doi:10.1029/98JB02125.
97. Archie, G.E. The Electrical Resistivity Log as an Aid in Determining Some Reservoir Characteristics. *Transactions of the AIME* **1942**, *146*, 54–62, doi:10.2118/942054-G.
98. Ioannidis, M.A.; Kwiecien, M.J.; Chatzis, I. Electrical Conductivity and Percolation Aspects of Statistically Homogeneous Porous Media. *Transp Porous Media* **1997**, *29*, 61–83.
99. Ghanbarian, B.; Hunt, A.G.; Ewing, R.P.; Skinner, T.E. Universal Scaling of the Formation Factor in Porous Media Derived by Combining Percolation and Effective Medium Theories. *Geophys Res Lett* **2014**, *41*, 3884–3890, doi:10.1002/2014GL060180.

100. Tosco, T.; Petrangeli Papini, M.; Cruz Viggi, C.; Sethi, R. Nanoscale Zerovalent Iron Particles for Groundwater Remediation: A Review. *J Clean Prod* **2014**, *77*, 10–21, doi:10.1016/j.jclepro.2013.12.026.
101. Cesano, F.; Uddin, M.J.; Lozano, K.; Zanetti, M.; Scarano, D. All-Carbon Conductors for Electronic and Electrical Wiring Applications. *Front Mater* **2020**, *7*, 541485, doi:10.3389/FMATS.2020.00219/BIBTEX.
102. Kulkarni, R.; Lingamdinne, L.P.; Koduru, J.R.; Karri, R.R.; Kailasa, S.K.; Mubarak, N.M.; Chang, Y.Y.; Dehghani, M.H. Exploring the Recent Cutting-Edge Applications of CNTs in Energy and Environmental Remediation: Mechanistic Insights and Remarkable Performance Advancements. *J Environ Chem Eng* **2024**, *12*, 113251, doi:10.1016/J.JECE.2024.113251.
103. Bianco, A.; Kostarelos, K.; Prato, M. Making Carbon Nanotubes Biocompatible and Biodegradable. *Chemical Communications* **2011**, *47*, 10182–10188, doi:10.1039/C1CC13011K.
104. Celzard, A.; Marêché, J.F.; Payot, F.; Furdin, G. Electrical Conductivity of Carbonaceous Powders. *Carbon N Y* **2002**, *40*, 2801–2815, doi:10.1016/S0008-6223(02)00196-3.
105. Del Prado-Audelo, M.L.; García Kerdan, I.; Escutia-Guadarrama, L.; Reyna-González, J.M.; Magaña, J.J.; Leyva-Gómez, G. Nanoremediation: Nanomaterials and Nanotechnologies for Environmental Cleanup. *Front Environ Sci* **2021**, *9*, 793765, doi:10.3389/FENVS.2021.793765/BIBTEX.
106. Xu, Y.; Bi, ·; Guy, L.; Zanli, L.; Chen, J.; Xu, Y.; Zanli, B.L.G.L.; Chen, · J New Consideration on the Application of Nano-Zero-Valent Iron (NZVI) in Groundwater Remediation: Refractions to Existing Technologies. *Journal of Nanoparticle Research 2024 26:1* **2024**, *26*, 1–24, doi:10.1007/S11051-023-05919-8.
107. Scida, K.; Stege, P.W.; Haby, G.; Messina, G.A.; García, C.D. Recent Applications of Carbon-Based Nanomaterials in Analytical Chemistry: Critical Review. *Anal Chim Acta* **2011**, *691*, 6–17, doi:10.1016/J.ACA.2011.02.025.
108. Bizmark, N.; Ioannidis, M.A. Effects of Ionic Strength on the Colloidal Stability and Interfacial Assembly of Hydrophobic Ethyl Cellulose Nanoparticles. *Langmuir* **2015**, *31*, 9282–9289, doi:10.1021/ACS.LANGMUIR.5B01857/ASSET/IMAGES/LARGE/LA-2015-01857R_0004.JPEG.
109. van Oss, C.J. The Extended DLVO Theory. *Interface Science and Technology* **2008**, *16*, 31–48, doi:10.1016/S1573-4285(08)00203-2.
110. Phenrat, T.; Saleh, N.; Sirk, K.; Tilton, R.D.; Lowry, G. V. Aggregation and Sedimentation of Aqueous Nanoscale Zerovalent Iron Dispersions. *Environ Sci Technol* **2007**, *41*, 284–290, doi:10.1021/es061349a.
111. Vecchia, E.D.; Coisson, M.; Appino, C.; Vinai, F.; Sethi, R. Magnetic Characterization and Interaction Modeling of Zerovalent Iron Nanoparticles for the Remediation of Contaminated Aquifers. *J Nanosci Nanotechnol* **2009**, *9*, 3210–3218, doi:10.1166/JNN.2009.047.
112. Falciglia, P.P.; Gagliano, E.; Scandura, P.; Bianco, C.; Tosco, T.; Sethi, R.; Varvaro, G.; Agostinelli, E.; Bongiorno, C.; Russo, A.; et al. Physico-Magnetic Properties and Dynamics of Magnetite (Fe3O4) Nanoparticles (MNPs) under the Effect of Permanent Magnetic Fields in Contaminated Water Treatment Applications. *Sep Purif Technol* **2022**, *296*, 121342, doi:10.1016/J.SEPPUR.2022.121342.
113. Bianco, C.; Mondino, F.; Casasso, A. Improved Delivery of Nanoscale Zero-Valent Iron Particles and Simplified Design Tools for Effective Aquifer Nanoremediation. *Water 2023, Vol. 15, Page 2303* **2023**, *15*, 2303, doi:10.3390/W15122303.
114. Tosco, T.; Gastone, F.; Sethi, R. Guar Gum Solutions for Improved Delivery of Iron Particles in Porous Media (Part 2): Iron Transport Tests and Modeling in Radial Geometry. *J Contam Hydrol* **2014**, *166*, 34–51, doi:10.1016/j.jconhyd.2014.06.014.

115. Tosco, T.; Sethi, R. Transport of Non-Newtonian Suspensions of Highly Concentrated Micro- and Nanoscale Iron Particles in Porous Media: A Modeling Approach. *Environ Sci Technol* **2010**, *44*, 9062–9068, doi:10.1021/ES100868N/SUPPL_FILE/ES100868N_SI_001.PDF.
116. Comba, S.; Sethi, R. Stabilization of Highly Concentrated Suspensions of Iron Nanoparticles Using Shear-Thinning Gels of Xanthan Gum. *Water Res* **2009**, *43*, 3717–3726, doi:10.1016/J.WATRES.2009.05.046.
117. Luna, M.; Gastone, F.; Tosco, T.; Sethi, R.; Velimirovic, M.; Gemoets, J.; Muyshondt, R.; Sapion, H.; Klaas, N.; Bastiaens, L. Pressure-Controlled Injection of Guar Gum Stabilized Microscale Zerovalent Iron for Groundwater Remediation. *J Contam Hydrol* **2015**, *181*, 46–58, doi:10.1016/J.JCONHYD.2015.04.007.
118. Velimirovic, M.; Tosco, T.; Uyttebroek, M.; Luna, M.; Gastone, F.; De Boer, C.; Klaas, N.; Sapion, H.; Eisenmann, H.; Larsson, P.O.; et al. Field Assessment of Guar Gum Stabilized Microscale Zerovalent Iron Particles for In-Situ Remediation of 1,1,1-Trichloroethane. *J Contam Hydrol* **2014**, *164*, 88–99, doi:10.1016/J.JCONHYD.2014.05.009.
119. Velimirovic, M.; Bianco, C.; Ferrantello, N.; Tosco, T.; Casasso, A.; Sethi, R.; Schmid, D.; Wagner, S.; Miyajima, K.; Klaas, N.; et al. A Large-Scale 3D Study on Transport of Humic Acid-Coated Goethite Nanoparticles for Aquifer Remediation. *Water 2020, Vol. 12, Page 1207* **2020**, *12*, 1207, doi:10.3390/W12041207.
120. Mohammadian, S.; Krok, B.; Fritzsche, A.; Bianco, C.; Tosco, T.; Cagigal, E.; Mata, B.; Gonzalez, V.; Diez-Ortiz, M.; Ramos, V.; et al. Field-Scale Demonstration of in Situ Immobilization of Heavy Metals by Injecting Iron Oxide Nanoparticle Adsorption Barriers in Groundwater. *J Contam Hydrol* **2021**, *237*, 103741, doi:10.1016/J.JCONHYD.2020.103741.
121. Krok, B.; Mohammadian, S.; Noll, H.M.; Surau, C.; Markwort, S.; Fritzsche, A.; Nachev, M.; Sures, B.; Meckenstock, R.U. Remediation of Zinc-Contaminated Groundwater by Iron Oxide in Situ Adsorption Barriers – From Lab to the Field. *Science of The Total Environment* **2022**, *807*, 151066, doi:10.1016/J.SCITOTENV.2021.151066.
122. Mahadevan, A.; Orpe, A. V.; Kudrolli, A.; Mahadevan, L. Flow-Induced Channelization in a Porous Medium. *Europhys Lett* **2012**, *98*, 58003, doi:10.1209/0295-5075/98/58003.
123. Fopa, R.D.; Bianco, C.; Archilha, N.L.; Moreira, A.C.; Pak, T. A Pore-Scale Investigation of the Effect of Nanoparticle Injection on Properties of Sandy Porous Media. *J Contam Hydrol* **2023**, *253*, 104126, doi:10.1016/J.JCONHYD.2022.104126.
124. Bianco, C.; Tosco, T.; Sethi, R. A 3-Dimensional Micro- and Nanoparticle Transport and Filtration Model (MNM3D) Applied to the Migration of Carbon-Based Nanomaterials in Porous Media. *J Contam Hydrol* **2016**, *193*, doi:10.1016/j.jconhyd.2016.08.006.
125. Yang, J.; Meng, L.; Guo, L. In Situ Remediation of Chlorinated Solvent-Contaminated Groundwater Using ZVI/Organic Carbon Amendment in China: Field Pilot Test and Full-Scale Application. *Environmental Science and Pollution Research* **2018**, *25*, 5051–5062, doi:10.1007/S11356-017-9903-7/FIGURES/7.
126. Beryani, A.; Alavi Moghaddam, M.R.; Tosco, T.; Bianco, C.; Hosseini, S.M.; Kowsari, E.; Sethi, R. Key Factors Affecting Graphene Oxide Transport in Saturated Porous Media. *Science of the Total Environment* **2020**, *698*, doi:10.1016/j.scitotenv.2019.134224.
127. Tosco, T.; Gastone, F.; Sethi, R. Guar Gum Solutions for Improved Delivery of Iron Particles in Porous Media (Part 2): Iron Transport Tests and Modeling in Radial Geometry. *J Contam Hydrol* **2014**, *166*, 34–51, doi:10.1016/J.JCONHYD.2014.06.014.
128. Torkzaban, S.; Bradford, S.A.; Vanderzalm, J.L.; Patterson, B.M.; Harris, B.; Prommer, H. Colloid Release and Clogging in Porous Media: Effects of Solution Ionic Strength and Flow Velocity. *J Contam Hydrol* **2015**, *181*, 161–171, doi:10.1016/J.JCONHYD.2015.06.005.

129. Yao, K.M.; Habibian, M.T.; O'Melia, C.R. Water and Waste Water Filtration: Concepts and Applications. *Environ Sci Technol* **1971**, *5*, 1105–1112, doi:10.1021/ES60058A005/ASSET/ES60058A005.FP.PNG_V03.
130. Šimůnek, J.; Šejna, M.; Saito, H.; Sakai, M.; van Genuchten, M.Th. *The HYDRUS-1D Software Package for Simulating the One-Dimensional Movement of Water, Heat, and Multiple Solutes in Variably-Saturated Media*; Riverside (California), 2009;
131. Tosco, T.; Sethi, R. Transport of Non-Newtonian Suspensions of Highly Concentrated Micro- And Nanoscale Iron Particles in Porous Media: A Modeling Approach. *Environ Sci Technol* **2010**, *44*, 9062–9068, doi:10.1021/es100868n.
132. Bianco, C.; Tosco, T.; Sethi, R. A 3-Dimensional Micro- and Nanoparticle Transport and Filtration Model (MNM3D) Applied to the Migration of Carbon-Based Nanomaterials in Porous Media. *J Contam Hydrol* **2016**, *193*, 10–20, doi:10.1016/j.jconhyd.2016.08.006.
133. Bianco, C.; Patiño Higuita, J.E.; Tosco, T.; Tiraferri, A.; Sethi, R. Controlled Deposition of Particles in Porous Media for Effective Aquifer Nanoremediation. *Sci Rep* **2017**, *7*, doi:10.1038/s41598-017-13423-y.
134. Meysman, F.J.R.; Cornelissen, R.; Trashin, S.; Bonné, R.; Martinez, S.H.; van der Veen, J.; Blom, C.J.; Karman, C.; Hou, J.L.; Eachambadi, R.T.; et al. A Highly Conductive Fibre Network Enables Centimetre-Scale Electron Transport in Multicellular Cable Bacteria. *Nature Communications 2019 10:1* **2019**, *10*, 1–8, doi:10.1038/s41467-019-12115-7.
135. Nielsen, L.P.; Risgaard-Petersen, N.; Fossing, H.; Christensen, P.B.; Sayama, M. Electric Currents Couple Spatially Separated Biogeochemical Processes in Marine Sediment. *Nature 2010 463:7284* **2010**, *463*, 1071–1074, doi:10.1038/nature08790.
136. Marzocchi, U.; Trojan, D.; Larsen, S.; Meyer, R.L.; Revsbech, N.P.; Schramm, A.; Nielsen, L.P.; Risgaard-Petersen, N. Electric Coupling between Distant Nitrate Reduction and Sulfide Oxidation in Marine Sediment. *The ISME Journal 2014 8:8* **2014**, *8*, 1682–1690, doi:10.1038/ismej.2014.19.
137. Pfeffer, C.; Larsen, S.; Song, J.; Dong, M.; Besenbacher, F.; Meyer, R.L.; Kjeldsen, K.U.; Schreiber, L.; Gorby, Y.A.; El-Naggar, M.Y.; et al. Filamentous Bacteria Transport Electrons over Centimetre Distances. *Nature 2012 491:7423* **2012**, *491*, 218–221, doi:10.1038/nature11586.
138. Trojan, D.; Schreiber, L.; Bjerg, J.T.; Bøggild, A.; Yang, T.; Kjeldsen, K.U.; Schramm, A. A Taxonomic Framework for Cable Bacteria and Proposal of the Candidate Genera Electrothrix and Electronema. *Syst Appl Microbiol* **2016**, *39*, 297–306, doi:10.1016/J.SYAPM.2016.05.006.
139. Plum-Jensen, L.E.; Schramm, A.; Marshall, I.P.G. First Single-Strain Enrichments of Electrothrix Cable Bacteria, Description of E. Aestuarii Sp. Nov. and E. Rattekaaiensis Sp. Nov., and Proposal of a Cable Bacteria Taxonomy Following the Rules of the SeqCode. *Syst Appl Microbiol* **2024**, *47*, 126487, doi:10.1016/J.SYAPM.2024.126487.
140. Malkin, S.Y.; Rao, A.M.F.; Seitaj, D.; Vasquez-Cardenas, D.; Zetsche, E.M.; Hidalgo-Martinez, S.; Boschker, H.T.S.; Meysman, F.J.R. Natural Occurrence of Microbial Sulphur Oxidation by Long-Range Electron Transport in the Seafloor. *The ISME Journal 2014 8:9* **2014**, *8*, 1843–1854, doi:10.1038/ismej.2014.41.
141. Marzocchi, U.; Bonaglia, S.; van de Velde, S.; Hall, P.O.J.; Schramm, A.; Risgaard-Petersen, N.; Meysman, F.J.R. Transient Bottom Water Oxygenation Creates a Niche for Cable Bacteria in Long-Term Anoxic Sediments of the Eastern Gotland Basin. *Environ Microbiol* **2018**, *20*, 3031–3041, doi:10.1111/1462-2920.14349.
142. Risgaard-Petersen, N.; Kristiansen, M.; Frederiksen, R.B.; Dittmer, A.L.; Bjerg, J.T.; Trojan, D.; Schreiber, L.; Damgaard, L.R.; Schramm, A.; Nielsen, L.P. Cable Bacteria in Freshwater

Sediments. *Appl Environ Microbiol* **2015**, *81*, 6003–6011, doi:10.1128/AEM.01064-15/SUPPL_FILE/ZAM999116535SO1.PDF.

143. Dam, A.S.; Marshall, I.P.G.; Risgaard-Petersen, N.; Burdorf, L.D.W.; Marzocchi, U. Effect of Salinity on Cable Bacteria Species Composition and Diversity. *Environ Microbiol* **2021**, *23*, 2605–2616, doi:10.1111/1462-2920.15484.
144. Müller, H.; Bosch, J.; Griebler, C.; Damgaard, L.R.; Nielsen, L.P.; Lueders, T.; Meckenstock, R.U. Long-Distance Electron Transfer by Cable Bacteria in Aquifer Sediments. *The ISME Journal 2016 10:8* **2016**, *10*, 2010–2019, doi:10.1038/ismej.2015.250.
145. Sandfeld, T.; Marzocchi, U.; Petro, C.; Schramm, A.; Risgaard-Petersen, N. Electrogenic Sulfide Oxidation Mediated by Cable Bacteria Stimulates Sulfate Reduction in Freshwater Sediments. *ISME J* **2020**, *14*, 1233–1246, doi:10.1038/S41396-020-0607-5.
146. Marzocchi, U.; Palma, E.; Rossetti, S.; Aulenta, F.; Scoma, A. Parallel Artificial and Biological Electric Circuits Power Petroleum Decontamination: The Case of Snorkel and Cable Bacteria. *Water Res* **2020**, *173*, 115520, doi:10.1016/J.WATRES.2020.115520.
147. Huang, Y.; Hu, W.; Dong, M.; Yang, Y.; Yang, X.; Huang, H.; Yang, S.; Jia, W.; Wang, B.; Xu, M. Cable Bacteria Accelerate the Anaerobic Removal of Pyrene in Black Odorous River Sediments. *J Hazard Mater* **2023**, *443*, 130305, doi:10.1016/J.JHAZMAT.2022.130305.
148. Kjeldsen, K.U.; Schreiber, L.; Thorup, C.A.; Boesen, T.; Bjerg, J.T.; Yang, T.; Dueholm, M.S.; Larsen, S.; Risgaard-Petersen, N.; Nierychlo, M.; et al. On the Evolution and Physiology of Cable Bacteria. *Proc Natl Acad Sci U S A* **2019**, *116*, 19116–19125, doi:10.1073/PNAS.1903514116/SUPPL_FILE/PNAS.1903514116.SD03.XLSX.
149. Reimers, C.E.; Li, C.; Graw, M.F.; Schrader, P.S.; Wolf, M. The Identification of Cable Bacteria Attached to the Anode of a Benthic Microbial Fuel Cell: Evidence of Long Distance Extracellular Electron Transport to Electrodes. *Front Microbiol* **2017**, *8*, 291990, doi:10.3389/FMICB.2017.02055/BIBTEX.
150. Bonné, R.; Marshall, I.P.G.; Bjerg, J.; Marzocchi, U.; Manca, J.; Nielsen, L.P.; Aiyer, K. Electrically Controlled Interaction between Cable Bacteria and Carbon Electrodes. *bioRxiv* **2023**, 2023.08.14.553267, doi:10.1101/2023.08.14.553267.
151. Bjerg, J.J.; Lustermans, J.J.M.; Marshall, I.P.G.; Mueller, A.J.; Brokjær, S.; Thorup, C.A.; Tataru, P.; Schmid, M.; Wagner, M.; Nielsen, L.P.; et al. Cable Bacteria with Electric Connection to Oxygen Attract Flocks of Diverse Bacteria. *Nature Communications 2023 14:1* **2023**, *14*, 1–8, doi:10.1038/s41467-023-37272-8.
152. Vasquez-Cardenas, D.; Van De Vossenberg, J.; Polerecky, L.; Malkin, S.Y.; Schauer, R.; Hidalgo-Martinez, S.; Confurius, V.; Middelburg, J.J.; Meysman, F.J.R.; Boschker, H.T.S. Microbial Carbon Metabolism Associated with Electrogenic Sulphur Oxidation in Coastal Sediments. *The ISME Journal 2015 9:9* **2015**, *9*, 1966–1978, doi:10.1038/ismej.2015.10.
153. Seigel, H.O. MATHEMATICAL FORMULATION AND TYPE CURVES FOR INDUCED POLARIZATION. *GEOPHYSICS* **1959**, *24*, 547–565, doi:10.1190/1.1438625.
154. Binley, A.; Hubbard, S.S.; Huisman, J.A.; Revil, A.; Robinson, D.A.; Singha, K.; Slater, L.D. The Emergence of Hydrogeophysics for Improved Understanding of Subsurface Processes over Multiple Scales. *Water Resour Res* **2015**, *51*, 3837–3866, doi:10.1002/2015WR017016.
155. Visconti, F.; de Paz, J.M. Electrical Conductivity Measurements in Agriculture: The Assessment of Soil Salinity. In *New Trends and Developments in Metrology*; InTech, 2016.
156. Groom, D. Common Misconceptions About Capacitively-Coupled Resistivity (CCR) What It Is and How It Works. In Proceedings of the Symposium on the Application of Geophysics to Engineering and Environmental Problems 2008; Environment and Engineering Geophysical Society, January 1 2008; Vol. 1, pp. 1345–1350.

157. Ünal, İ.; Kabaş, Ö.; Sözer, S. Real-Time Electrical Resistivity Measurement and Mapping Platform of the Soils with an Autonomous Robot for Precision Farming Applications. *Sensors (Basel)* **2020**, *20*, 251, doi:10.3390/s20010251.
158. Fuller, B.D.; Ward, S.H. Linear System Description of the Electrical Parameters of Rocks. *IEEE Transactions on Geoscience Electronics* **1970**, *8*, 7–18, doi:10.1109/TGE.1970.271447.
159. Winsauer, W.O.; McCardell, W.M. Ionic Double-Layer Conductivity in Reservoir Rock. *Journal of Petroleum Technology* **1953**, *5*, 129–134, doi:10.2118/953129-G.
160. Waxman, M.H.; Smits, L.J.M. Electrical Conductivities in Oil-Bearing Shaly Sands. *Society of Petroleum Engineers Journal* **1968**, *8*, 107–122, doi:10.2118/1863-A.
161. Archie, G.E. Introduction to Petrophysics of Reservoir Rocks. *Am Assoc Pet Geol Bull* **1950**, *34*, 943–961.
162. Atekwana, E.A.; Atekwana, E.A. Geophysical Signatures of Microbial Activity at Hydrocarbon Contaminated Sites: A Review. *Surv Geophys* **2010**, *31*, 247–283, doi:10.1007/S10712-009-9089-8/FIGURES/18.
163. Kemna, A.; Binley, A.; Cassiani, G.; Niederleithinger, E.; Revil, A.; Slater, L.; Williams, K.H.; Orozco, A.F.; Haegel, F.H.; Hördt, A.; et al. An Overview of the Spectral Induced Polarization Method for Near-Surface Applications. *Near Surface Geophysics* **2012**, *10*, 453–468, doi:10.3997/1873-0604.2012027.
164. Leroy, P.; Revil, A. A Mechanistic Model for the Spectral Induced Polarization of Clay Materials. *J Geophys Res Solid Earth* **2009**, *114*, 10202, doi:10.1029/2008JB006114.
165. Prodan, E.; Prodan, C.; Miller, J.H. The Dielectric Response of Spherical Live Cells in Suspension: An Analytic Solution. *Biophys J* **2008**, *95*, 4174–4182, doi:10.1529/biophysj.108.137042.
166. Zhao, Z.; Li, Y.; Zhang, Y.; Lovley, D.R. Sparking Anaerobic Digestion: Promoting Direct Interspecies Electron Transfer to Enhance Methane Production. *iScience* **2020**, *23*, doi:10.1016/J.ISCI.2020.101794/ATTACHMENT/3B2E79E2-D142-4850-B1DA-7002AACDF0CC/MMC3.XLS.
167. Barsoukov, E.; Macdonald, J.R. *Impedance Spectroscopy: Theory, Experiment, and Applications*; John Wiley and Sons, 2005; ISBN 0471647497.
168. Dafter, M. Electrochemical Impedance Spectroscopy of Soils. In Proceedings of the 8th International Corrosion Congress ; 2011; pp. 1796–1806.
169. Li, X.; Wang, X.; Zhao, Q.; Zhang, Y.; Zhou, Q.; Binions, R. In Situ Representation of Soil/Sediment Conductivity Using Electrochemical Impedance Spectroscopy., doi:10.3390/s16050625.
170. Shuquan, P.; Fan, W.; Ling, F. Study on Electrochemical Impedance Response of Sulfate Saline Soil. *Int J Electrochem Sci* **2019**, *14*, 8611–8623, doi:10.20964/2019.09.30.
171. Sun, F.; Chen, Z.; Bai, X.; Wang, Y.; Liu, X.; He, B.; Han, P. Theoretical and Experimental Bases for the Equivalent Circuit Model for Interpretation of Silty Soil at Different Temperatures. *Heliyon* **2023**, *9*, e12652, doi:10.1016/j.heliyon.2022.e12652.
172. Guglielmi, S.; Pirone, M.; Amatucci, N.; Cesaro, U.; D'Arco, M.; Urciuoli, G. A Prototype for Water Content Measurement in Partially Saturated Soils. *E3S Web of Conferences* **2023**, *382*, 22005, doi:10.1051/E3SCONF/202338222005.
173. Dahlin, T.; Zhou, B. A Numerical Comparison of 2D Resistivity Imaging with 10 Electrode Arrays. *Geophys Prospect* **2004**, *52*, 379–398, doi:10.1111/J.1365-2478.2004.00423.X.
174. Wagner, F.M.; Günther, T.; Schmidt-Hattenberger, C.; Maurer, H. Constructive Optimization of Electrode Locations for Target-Focused Resistivity Monitoring. *https://doi.org/10.1190/geo2014-0214.1* **2015**, *80*, E29–E40, doi:10.1190/GEO2014-0214.1.

175. Daily, W.; Ramirez, A.; LaBrecque, D.; Nitao, J. Electrical Resistivity Tomography of Vadose Water Movement. *Water Resour Res* **1992**, *28*, 1429–1442, doi:10.1029/91WR03087.
176. Binley, A.; Henry-Poulter, S.; Shaw, B. Examination of Solute Transport in an Undisturbed Soil Column Using Electrical Resistance Tomography. *Water Resour Res* **1996**, *32*, 763–769, doi:10.1029/95WR02995.
177. Ramirez, A.; Daily, W.; LaBrecque, D.; Owen, E.; Chesnut, D. Monitoring an Underground Steam Injection Process Using Electrical Resistance Tomography. *Water Resour Res* **1993**, *29*, 73–87, doi:10.1029/92WR01608.
178. LaBrecque, D.J.; Ramirez, A.L.; Daily, W.D.; Binley, A.M.; Schima, S.A. ERT Monitoring of Environmental Remediation Processes. *Meas Sci Technol* **1996**, *7*, 375, doi:10.1088/0957-0233/7/3/019.
179. Storz, H.; Storz, W.; Jacobs, F. Electrical Resistivity Tomography to Investigate Geological Structures of the Earth's Upper Crust. *Geophys Prospect* **2000**, *48*, 455–471, doi:10.1046/J.1365-2478.2000.00196.X.
180. Vanella, D.; Cassiani, G.; Busato, L.; Boaga, J.; Barbagallo, S.; Binley, A.; Consoli, S. Use of Small Scale Electrical Resistivity Tomography to Identify Soil-Root Interactions during Deficit Irrigation. *J Hydrol (Amst)* **2018**, *556*, 310–324, doi:10.1016/J.JHYDROL.2017.11.025.
181. Uhlemann, S.; Peruzzo, L.; Chou, C.; Williams, K.H.; Wielandt, S.; Wang, C.; Falco, N.; Wu, Y.; Carr, B.; Meldrum, P.; et al. Variations in Bedrock and Vegetation Cover Modulate Subsurface Water Flow Dynamics of a Mountainous Hillslope. *Water Resour Res* **2024**, *60*, e2023WR036137, doi:10.1029/2023WR036137.
182. Caterina, D.; Flores Orozco, A.; Nguyen, F. Long-Term ERT Monitoring of Biogeochemical Changes of an Aged Hydrocarbon Contamination. *J Contam Hydrol* **2017**, *201*, 19–29, doi:10.1016/J.JCONHYD.2017.04.003.
183. Clément, R.; Descloitres, M.; Günther, T.; Oxarango, L.; Morra, C.; Laurent, J.P.; Gourc, J.P. Improvement of Electrical Resistivity Tomography for Leachate Injection Monitoring. *Waste Management* **2010**, *30*, 452–464, doi:10.1016/J.WASMAN.2009.10.002.
184. Bichet, V.; Grisey, E.; Aleya, L. Spatial Characterization of Leachate Plume Using Electrical Resistivity Tomography in a Landfill Composed of Old and New Cells (Belfort, France). *Eng Geol* **2016**, *211*, 61–73, doi:10.1016/J.ENGGEO.2016.06.026.
185. Georgaki, I.; Soupios, P.; Sakkas, N.; Ververidis, F.; Trantas, E.; Vallianatos, F.; Manios, T. Evaluating the Use of Electrical Resistivity Imaging Technique for Improving CH4 and CO2 Emission Rate Estimations in Landfills. *Science of The Total Environment* **2008**, *389*, 522–531, doi:10.1016/J.SCITOTENV.2007.08.033.
186. André, L.; Lamy, E.; Lutz, P.; Pernier, M.; Lespinard, O.; Pauss, A.; Ribeiro, T. Electrical Resistivity Tomography to Quantify in Situ Liquid Content in a Full-Scale Dry Anaerobic Digestion Reactor. *Bioresour Technol* **2016**, *201*, 89–96, doi:10.1016/J.BIORTECH.2015.11.033.
187. Sainato, C.M.; Losinno, B.N.; Malleville, H.J. Electrical Resistivity Tomography Applied to Detect Contamination on a Dairy Farm in the Pampean Region, Argentina. *Near Surface Geophysics* **2010**, *8*, 163–171, doi:10.3997/1873-0604.2009060.
188. Helene, L.P.I.; Moreira, C.A.; Bovi, R.C. Identification of Leachate Infiltration and Its Flow Pathway in Landfill by Means of Electrical Resistivity Tomography (ERT). *Environ Monit Assess* **2020**, *192*, 1–10, doi:10.1007/S10661-020-8206-5/FIGURES/5.
189. Simyrdanis, K.; Papadopoulos, N.; Soupios, P.; Kirkou, S.; Tsourlos, P. Characterization and Monitoring of Subsurface Contamination from Olive Oil Mills' Waste Waters Using Electrical Resistivity Tomography. *Science of The Total Environment* **2018**, *637–638*, 991–1003, doi:10.1016/J.SCITOTENV.2018.04.348.

190. Xia, T.; Ma, M.; Huisman, J.A.; Zheng, C.; Gao, C.; Mao, D. Monitoring of In-Situ Chemical Oxidation for Remediation of Diesel-Contaminated Soil with Electrical Resistivity Tomography. *J Contam Hydrol* **2023**, *256*, 104170, doi:10.1016/J.JCONHYD.2023.104170.
191. Rosales, R.M.; Martínez-Pagan, P.; Faz, A.; Moreno-Cornejo, J. Environmental Monitoring Using Electrical Resistivity Tomography (ERT) in the Subsoil of Three Former Petrol Stations in SE of Spain. *Water Air Soil Pollut* **2012**, *223*, 3757–3773, doi:10.1007/S11270-012-1146-0/FIGURES/9.
192. Mao, D.; Lu, L.; Revil, A.; Zuo, Y.; Hinton, J.; Ren, Z.J. Geophysical Monitoring of Hydrocarbon-Contaminated Soils Remediated with a Bioelectrochemical System. *Environ Sci Technol* **2016**, *50*, 8205–8213, doi:10.1021/ACS.EST.6B00535/ASSET/IMAGES/MEDIUM/ES-2016-005359_0007.GIF.
193. Cassiani, G.; Binley, A.; Kemna, A.; Wehrer, M.; Orozco, A.F.; Deiana, R.; Boaga, J.; Rossi, M.; Dietrich, P.; Werban, U.; et al. Noninvasive Characterization of the Trecate (Italy) Crude-Oil Contaminated Site: Links between Contamination and Geophysical Signals. *Environmental Science and Pollution Research* **2014**, *21*, 8914–8931, doi:10.1007/S11356-014-2494-7/FIGURES/16.
194. Li, Z. ping; Liu, Y.; Zhao, G. zhang; Liu, S. kang; Liu, W. hui LNAPL Migration Processes Based on Time-Lapse Electrical Resistivity Tomography. *J Contam Hydrol* **2023**, *259*, 104260, doi:10.1016/J.JCONHYD.2023.104260.
195. Ciampi, P.; Esposito, C.; Cassiani, G.; Deidda, G.P.; Rizzetto, P.; Papini, M.P. A Field-Scale Remediation of Residual Light Non-Aqueous Phase Liquid (LNAPL): Chemical Enhancers for Pump and Treat. *Environmental Science and Pollution Research* **2021**, *28*, 35286–35296, doi:10.1007/S11356-021-14558-2/FIGURES/7.
196. Goes, B.J.M.; Meekes, J.A.C. An Effective Electrode Configuration for the Detection of DNAPLs with Electrical Resistivity Tomography. *https://doi.org/10.4133/JEEG9.3.127* **2012**, *9*, 127–141, doi:10.4133/JEEG9.3.127.
197. Trento, L.M.; Tsourlos, P.; Gerhard, J.I. Time-Lapse Electrical Resistivity Tomography Mapping of DNAPL Remediation at a STAR Field Site. *J Appl Geophy* **2021**, *184*, 104244, doi:10.1016/J.JAPPGEO.2020.104244.
198. Cassidy, D.P.; Jr., D.D.W.; Sauck, W.; Atekwana, E.; Rossbach, S.; Duris, J. The Effects of LNAPL Biodegradation Products on Electrical Conductivity Measurements. *https://doi.org/10.4133/JEEG6.1.47* **2012**, *6*, 47–52, doi:10.4133/JEEG6.1.47.
199. Yabusaki, S.B.; Wilkins, M.J.; Fang, Y.; Williams, K.H.; Arora, B.; Bargar, J.; Beller, H.R.; Bouskill, N.J.; Brodie, E.L.; Christensen, J.N.; et al. Water Table Dynamics and Biogeochemical Cycling in a Shallow, Variably-Saturated Floodplain. *Environ Sci Technol* **2017**, *51*, 3307–3317, doi:10.1021/ACS.EST.6B04873/ASSET/IMAGES/LARGE/ES-2016-048735_0007.JPEG.
200. Ciampi, P.; Esposito, C.; Cassiani, G.; Deidda, G.P.; Flores-Orozco, A.; Rizzetto, P.; Chiappa, A.; Bernabei, M.; Gardon, A.; Petrangeli Papini, M. Contamination Presence and Dynamics at a Polluted Site: Spatial Analysis of Integrated Data and Joint Conceptual Modeling Approach. *J Contam Hydrol* **2022**, *248*, 104026, doi:10.1016/J.JCONHYD.2022.104026.
201. Tarasov, A.; Titov, K. Relaxation Time Distribution from Time Domain Induced Polarization Measurements. *Geophys J Int* **2007**, *170*, 31–43, doi:10.1111/J.1365-246X.2007.03376.X/2/170-1-31-TBL002.JPEG.
202. Fiandaca, G.; Ramm, J.; Binley, A.; Gazoty, A.; Christiansen, A.V.; Auken, E. Resolving Spectral Information from Time Domain Induced Polarization Data through 2-D Inversion. *Geophys J Int* **2013**, *192*, 631–646, doi:10.1093/GJI/GGS060.

203. Revil, A.; Binley, A.; Mejus, L.; Kessouri, P. Predicting Permeability from the Characteristic Relaxation Time and Intrinsic Formation Factor of Complex Conductivity Spectra. *Water Resour Res* **2015**, *51*, 6672–6700, doi:10.1002/2015WR017074.
204. Zarroca, M.; Rodríguez, R.; Corral, I.; Revil, A.; Vaudelet, P.; Su, Z.; Chen, R. Induced Polarization as a Tool to Assess Mineral Deposits: A Review. *Minerals 2022, Vol. 12, Page 571* **2022**, *12*, 571, doi:10.3390/MIN12050571.
205. Pelton, W.H.; Ward, S.H.; Hallof, P.G.; Sill, W.R.; Nelson, P.H. Mineral Discrimination and Removal of Inductive Coupling with Multifrequency IP. *Geophysics* **1978**, *43*, 588–609, doi:10.1190/1.1440839.
206. Martin, T.; Weller, A.; Behling, L. Desaturation Effects of Pyrite–Sand Mixtures on Induced Polarization Signals. *Geophys J Int* **2021**, *228*, 275–290, doi:10.1093/GJI/GGAB333.
207. Slater, L.D.; Choi, J.; Wu, Y. Electrical Properties of Iron-Sand Columns: Implications for Induced Polarization Investigation and Performance Monitoring of Iron-Wall Barriers. *Geophysics* **2005**, *70*, doi:10.1190/1.1990218.
208. Hupfer, S.; Martin, T.; Weller, A.; Günther, T.; Kuhn, K.; Djotsa Nguimeya Ngninjio, V.; Noell, U. Polarization Effects of Unconsolidated Sulphide-Sand-Mixtures. *J Appl Geophy* **2016**, *135*, 456–465, doi:10.1016/J.JAPPGEO.2015.12.003.
209. Gurin, G.; Titov, K.; Ilyin, Y. Induced Polarization of Rocks Containing Metallic Particles: Evidence of Passivation Effect. *Geophys Res Lett* **2019**, *46*, 670–677, doi:10.1029/2018GL080107.
210. Wong, J. An Electrochemical Model of the Induced-Polarization Phenomenon in Disseminated Sulfide Ores. *Geophysics* **1979**, *44*, 1245–1265, doi:10.1190/1.1441005.
211. Bücker, M.; Orozco, A.F.; Kemna, A. Electrochemical Polarization around Metallic Particles — Part 1: The Role of Diffuse-Layer and Volume-Diffusion Relaxation. *https://doi.org/10.1190/geo2017-0401.1* **2018**, *83*, E203–E217, doi:10.1190/GEO2017-0401.1.
212. Bücker, M.; Undorf, S.; Flores Orozco, A.; Kemna, A. Electrochemical Polarization around Metallic Particles — Part 2: The Role of Diffuse Surface Charge. *https://doi.org/10.1190/geo2018-0150.1* **2019**, *84*, E57–E73, doi:10.1190/GEO2018-0150.1.
213. Gurin, G.; Titov, K.; Ilyin, Y.; Fomina, E. Spectral Induced Polarization in Anisotropic Rocks with Electrically Conductive Inclusions: Synthetic Model Study. *Geophys J Int* **2021**, *224*, 871–895, doi:10.1093/GJI/GGAA480.
214. Personna, Y.R.; Ntarlagiannis, D.; Slater, L.; Yee, N.; O'Brien, M.; Hubbard, S. Spectral Induced Polarization and Electrodic Potential Monitoring of Microbially Mediated Iron Sulfide Transformations. *J Geophys Res Biogeosci* **2008**, *113*, 2020, doi:10.1029/2007JG000614.
215. Williams, K.H.; Kemna, A.; Wilkins, M.J.; Druhan, J.; Arntzen, E.; N'Guessan, A.L.; Long, P.E.; Hubbard, S.S.; Banfield, J.F. Geophysical Monitoring of Coupled Microbial and Geochemical Processes during Stimulated Subsurface Bioremediation. *Environ Sci Technol* **2009**, *43*, 6717–6723, doi:10.1021/ES900855J/SUPPL_FILE/ES900855J_SI_001.PDF.
216. Flores-Orozco, A.; Gallistl, J.; Steiner, M.; Brandstätter, C.; Fellner, J. Mapping Biogeochemically Active Zones in Landfills with Induced Polarization Imaging: The Heferlbach Landfill. *Waste Management* **2020**, *107*, 121–132, doi:10.1016/J.WASMAN.2020.04.001.
217. Wu, Y.; Peruzzo, L. Effects of Salinity and PH on the Spectral Induced Polarization Signals of Graphite Particles. *Geophys J Int* **2020**, *221*, 1532–1541, doi:10.1093/GJI/GGAA087.
218. Atekwana, E.A.; Slater, L.D. Biogeophysics: A New Frontier in Earth Science Research. *Reviews of Geophysics* **2009**, *47*, doi:10.1029/2009RG000285.

219. Foster, K.; Schwan, H. Dielectric Properties of Tissues and Biological Materials: A Critical Review. *Crit Rev Biomed Eng* **1989**.
220. Revil, A.; Atekwana, E.; Zhang, C.; Jardani, A.; Smith, S. A New Model for the Spectral Induced Polarization Signature of Bacterial Growth in Porous Media. *Water Resour Res* **2012**, *48*, doi:10.1029/2012WR011965.
221. Schwarz, G. A Theory of the Low-Frequency Dielectric Dispersion of Colloidal Particles in Electrolyte Solution. *Journal of Physical Chemistry* **1962**, *66*, 2636–2642, doi:10.1021/J100818A067/ASSET/J100818A067.FP.PNG_V03.
222. Mellage, A.; Smeaton, C.M.; Furman, A.; Atekwana, E.A.; Rezanezhad, F.; Van Cappellen, P. Linking Spectral Induced Polarization (SIP) and Subsurface Microbial Processes: Results from Sand Column Incubation Experiments. *Environ Sci Technol* **2018**, *52*, 2081–2090, doi:10.1021/ACS.EST.7B04420/SUPPL_FILE/ES7B04420_SI_002.PDF.
223. Zhang, C.; Revil, A.; Fujita, Y.; Munakata-Marr, J.; Redden, G. Quadrature Conductivity: A Quantitative Indicator of Bacterial Abundance in Porous Media. *https://doi.org/10.1190/geo2014-0107.1* **2014**, *79*, D363–D375, doi:10.1190/GEO2014-0107.1.
224. Abdel Aal, G.Z.A.; Slater, L.D.; Atekwana, E.A. Induced-Polarization Measurements on Unconsolidated Sediments from a Site of Active Hydrocarbon Biodegradation. *Geophysics* **2006**, *71*, doi:10.1190/1.2187760.
225. Peruzzo, L.; Liu, X.; Chou, C.; Blancaflor, E.B.; Zhao, H.; Ma, X.F.; Mary, B.; Iván, V.; Weigand, M.; Wu, Y. Three-Channel Electrical Impedance Spectroscopy for Field-Scale Root Phenotyping. *The Plant Phenome Journal* **2021**, *4*, e20021, doi:10.1002/PPJ2.20021.
226. Mary, B.; Abdulsamad, F.; Saracco, G.; Peyras, L.; Vennetier, M.; Mériaux, P.; Camerlynck, C. Improvement of Coarse Root Detection Using Time and Frequency Induced Polarization: From Laboratory to Field Experiments. *Plant Soil* **2017**, *417*, 243–259, doi:10.1007/S11104-017-3255-4/FIGURES/9.
227. Zhu, F.; Leonard, E.F.; Levin, N.W. Bioelectrical Impedance and The Frequency Dependent Current Conduction Through Biological Tissues: A Short Review. *IOP Conf Ser Mater Sci Eng* **2018**, *331*, 012005, doi:10.1088/1757-899X/331/1/012005.
228. Katona, T.; Gilfedder, B.S.; Frei, S.; Bücker, M.; Flores-Orozco, A. High-Resolution Induced Polarization Imaging of Biogeochemical Carbon Turnover Hotspots in a Peatland. *Biogeosciences* **2021**, *18*, 4039–4058, doi:10.5194/BG-18-4039-2021.
229. Peruzzo, L.; Schmutz, M.; Franceschi, M.; Wu, Y.; Hubbard, S.S. The Relative Importance of Saturated Silica Sand Interfacial and Pore Fluid Geochemistry on the Spectral Induced Polarization Response. *J Geophys Res Biogeosci* **2018**, *123*, 1702–1718, doi:10.1029/2017JG004364.
230. Skold, M.; Revil, A.; Vaudelet, P. The PH Dependence of Spectral Induced Polarization of Silica Sands: Experiment and Modeling. *Geophys Res Lett* **2011**, *38*, doi:10.1029/2011GL047748.
231. Wu, Y.; Hubbard, S.; Williams, K.H.; Ajo-Franklin, J. On the Complex Conductivity Signatures of Calcite Precipitation. *J Geophys Res Biogeosci* **2010**, *115*, 0–04, doi:10.1029/2009JG001129.
232. Saneiyan, S.; Ntarlagiannis, D.; Ohan, J.; Lee, J.; Colwell, F.; Burns, S. Induced Polarization as a Monitoring Tool for In-Situ Microbial Induced Carbonate Precipitation (MICP) Processes. *Ecol Eng* **2019**, *127*, 36–47, doi:10.1016/J.ECOLENG.2018.11.010.
233. Weller, A.; Slater, L. Salinity Dependence of Complex Conductivity of Unconsolidated and Consolidated Materials: Comparisons with Electrical Double Layer Models. *Geophysics* **2012**, *77*, doi:10.1190/GEO2012-0030.1.

234. Slater, L.D.; Lesmes, D. IP Interpretation in Environmental Investigations. *Geophysics* **2002**, *67*, 77–88, doi:10.1190/1.1451353.
235. Schmutz, M.; Revil, A.; Vaudelet, P.; Batzle, M.; Viñao, P.F.; Werkema, D.D. Influence of Oil Saturation upon Spectral Induced Polarization of Oil-Bearing Sands. *Geophys J Int* **2010**, *183*, 211–224, doi:10.1111/J.1365-246X.2010.04751.X/2/183-1-211-FIG011.JPEG.
236. BÖRNER, F.; GRUHNE, M.; SCHÖN, J. CONTAMINATION INDICATIONS DERIVED FROM ELECTRICAL PROPERTIES IN THE LOW FREQUENCY RANGE1. *Geophys Prospect* **1993**, *41*, 83–98, doi:10.1111/J.1365-2478.1993.TB00566.X.
237. Deng, Y.; Shi, X.; Zhang, Z.; Sun, Y.; Wu, J.; Qian, J. Application of Spectral Induced Polarization for Characterizing Surfactant-Enhanced DNAPL Remediation in Laboratory Column Experiments. *J Contam Hydrol* **2020**, *230*, 103603, doi:10.1016/J.JCONHYD.2020.103603.
238. PARASNIS, D.S. THREE-DIMENSIONAL ELECTRIC MISE-A-LA-MASSE SURVEY OF AN IRREGULAR LEAD-ZINC-COPPER DEPOSIT IN CENTRAL SWEDEN *. *Geophys Prospect* **1967**, *15*, 407–437, doi:10.1111/J.1365-2478.1967.TB01796.X.
239. Ling, C.; Revil, A.; Abdulsamad, F.; Qi, Y.; Soueid Ahmed, A.; Shi, P.; Nicaise, S.; Peyras, L. Leakage Detection of Water Reservoirs Using a Mise-à-La-Masse Approach. *J Hydrol (Amst)* **2019**, *572*, 51–65, doi:10.1016/J.JHYDROL.2019.02.046.
240. De Carlo, L.; Perri, M.T.; Caputo, M.C.; Deiana, R.; Vurro, M.; Cassiani, G. Characterization of a Dismissed Landfill via Electrical Resistivity Tomography and Mise-à-La-Masse Method. *J Appl Geophy* **2013**, *98*, 1–10, doi:10.1016/J.JAPPGEO.2013.07.010.
241. Osiensky, J.L.; Donaldson, P.R. Electrical Flow through an Aquifer for Contaminant Source Leak Detection and Delineation of Plume Evolution. *J Hydrol (Amst)* **1995**, *169*, 243–263, doi:10.1016/0022-1694(94)02610-N.
242. Osiensky, J.L.; Donaldson, P.R. A Modified Mise-A'-La-Masse Method for Contaminant Plume Delineation. *Groundwater* **1994**, *32*, 448–457, doi:10.1111/J.1745-6584.1994.TB00662.X.
243. Osiensky, J.L. Ground Water Modeling of Mise-a-La-Masse Delineation of Contaminated Ground Water Plumes. *J Hydrol (Amst)* **1997**, *197*, 146–165, doi:10.1016/S0022-1694(96)03279-9.
244. Perri, M.T.; De Vita, P.; Masciale, R.; Portoghese, I.; Chirico, G.B.; Cassiani, G. Time-Lapse Mise-á-La-Masse Measurements and Modeling for Tracer Test Monitoring in a Shallow Aquifer. *J Hydrol (Amst)* **2018**, *561*, 461–477, doi:10.1016/J.JHYDROL.2017.11.013.
245. Peruzzo, L.; Chou, C.; Wu, Y.; Schmutz, M.; Mary, B.; Wagner, F.M.; Petrov, P.; Newman, G.; Blancaflor, E.B.; Liu, X.; et al. Imaging of Plant Current Pathways for Non-Invasive Root Phenotyping Using a Newly Developed Electrical Current Source Density Approach. *Plant Soil* **2020**, *450*, 567–584, doi:10.1007/S11104-020-04529-W/FIGURES/10.
246. Binley, A.; Daily, W.; Ramirez, A. Detecting Leaks from Environmental Barriers Using Electrical Current Imaging. *https://doi.org/10.4133/JEEG2.1.11* **2008**, *2*, 11–19, doi:10.4133/JEEG2.1.11.
247. Mary, B.; Peruzzo, L.; Wu, Y.; Cassiani, G. Advanced Potential Field Analysis Applied to Mise-à-La-Masse Surveys for Leakage Detection. *J Geophys Res Solid Earth* **2022**, *127*, e2022JB024747, doi:10.1029/2022JB024747.
248. Mary, B.; Vanella, D.; Consoli, S.; Cassiani, G. Assessing the Extent of Citrus Trees Root Apparatus under Deficit Irrigation via Multi-Method Geo-Electrical Imaging. *Scientific Reports 2019 9:1* **2019**, *9*, 1–10, doi:10.1038/s41598-019-46107-w.
249. Boaga, J. The Use of FDEM in Hydrogeophysics: A Review. *J Appl Geophy* **2017**, *139*, 36–46, doi:10.1016/J.JAPPGEO.2017.02.011.

250. Deiana, R.; Cassiani, G.; Kemna, A.; Villa, A.; Bruno, V.; Bagliani, A. An Experiment of Non-Invasive Characterization of the Vadose Zone via Water Injection and Cross-Hole Time-Lapse Geophysical Monitoring. *Near Surface Geophysics* **2007**, *5*, 183–194, doi:10.3997/1873-0604.2006030.
251. Wang, T.P.; Chen, C.C.; Tong, L.T.; Chang, P.Y.; Chen, Y.C.; Dong, T.H.; Liu, H.C.; Lin, C.P.; Yang, K.H.; Ho, C.J.; et al. Applying FDEM, ERT and GPR at a Site with Soil Contamination: A Case Study. *J Appl Geophy* **2015**, *121*, 21–30, doi:10.1016/J.JAPPGEO.2015.07.005.
252. Lanz, E.; Maurer, H.; Green, A.G. Refraction Tomography over a Buried Waste Disposal Site. *Geophysics* **1998**, *63*, 1414–1433, doi:10.1190/1.1444443.
253. Nivorlis, A.; Dahlin, T.; Rossi, M.; Höglund, N.; Sparrenbom, C. Multidisciplinary Characterization of Chlorinated Solvents Contamination and In-Situ Remediation with the Use of the Direct Current Resistivity and Time-Domain Induced Polarization Tomography. *Geosciences 2019, Vol. 9, Page 487* **2019**, *9*, 487, doi:10.3390/GEOSCIENCES9120487.
254. Hubbard, S.S.; Williams, K.; Conrad, M.E.; Faybishenko, B.; Peterson, J.; Chen, J.; Long, P.; Hazen, T. Geophysical Monitoring of Hydrological and Biogeochemical Transformations Associated with Cr(VI) Bioremediation. *Environ Sci Technol* **2008**, *42*, 3757–3765, doi:10.1021/ES071702S/SUPPL_FILE/ES071702S-FILE002.PDF.
255. Cai, J.; Wei, W.; Hu, X.; Wood, D.A. Electrical Conductivity Models in Saturated Porous Media: A Review. *Earth Sci Rev* **2017**, *171*, 419–433, doi:10.1016/j.earscirev.2017.06.013.

Figure Captions

Figure 1. a, The creation of a "diffuse electro-conductive zone (DECZ)" within a contaminated aquifer through the injection of iron- or carbon-based materials. **b**, Extending the radius of influence (ROI) of anodes and cathodes exploiting the DECZ concept. **c**, Promoting the anaerobic, direct interspecies electron transfer (DIET)-based, cooperative degradation of reduced pollutants under methanogenic or sulfate-reducing conditions by exploiting the DECZ concept.

Figure 2. The apparent effect of distance from the anode on the fold increase of petroleum-hydrocarbon bioelectrochemical removal relative to open circuit potential (OCP) control experiments [79].

Figure 3. Injection strategies that can be applied for subsurface delivery of conductive micro and nanoparticles: **a**, permeation injection; **b**, fracturing injection.

Figure 4. The schematic of the four-probe configuration to measure soil conductivity [157]. DC, direct current.

Table 1. Metal- and carbon-based conductive materials: electrical properties, toxicological parameters and concentration limits in groundwater.

Compound	Concentration limit in groundwater[a] ($\mu g\ L^{-1}$)	Oral chronic reference dose[b] ($mg\ kg^{-1}\ d^{-1}$)	Oral slope factor[b] ($mg\ kg^{-1}\ d^{-1}$)	Conductivity ($S\ m^{-1}$)	Resistivity ($\Omega\ m$)	Oxide conductivity ($S\ m^{-1}$)	Oxide resistivity ($\Omega\ m$)
Metals							
Aluminum	200	1	-	3.5×10^{7}	2.8×10^{-8}	$\sim10^{-14}$	$\sim10^{14}$
Antimony	5	4×10^{-4}	-	2.5×10^{4}	4.0×10^{-5}	-	-
Arsenic	10	3×10^{-4}	1.5	3.3×10^{4}	3.0×10^{-5}	-	-
Beryllium	4	2×10^{-3}	-	2.5×10^{7}	4×10^{-8}	-	-
Cadmium	5	5×10^{-4}	-	1.3×10^{7}	7.3×10^{-8}	-	-
Chromium	50	3×10^{-3}	5×10^{-1}	7.9×10^{6}	1.25×10^{-7}	-	-
Cobalt	50	3×10^{-4}	-	1.7×10^{7}	6.24×10^{-8}	-	-
Copper	1000	4×10^{-2}	-	5.9×10^{7}	1.68×10^{-8}	$\sim10^{-5}$ to 10^{-6}	$\sim10^{5}$ to 10^{6}
Gold	-	-	-	4.1×10^{7}	2.44×10^{-8}	-	-
Iron	200	7×10^{-1}	-	1.0×10^{7}	1.0×10^{-7}	$\sim10^{-1}$ to 10^{-3}	~10 to 10^{3}
Lead	10	-	8.5×10^{-3}	4.8×10^{6}	2.2×10^{-7}	-	-
Manganese	50	1.4×10^{-1}	-	6.9×10^{5}	1.44×10^{-6}	-	-
Mercury	1	1.6×10^{-4}	-	1.0×10^{6}	1.0×10^{-6}	-	-
Nickel	20	2×10^{-2}	-	1.4×10^{7}	6.9×10^{-8}	-	-
Platinum	-	-	-	9.4×10^{6}	10.6×10^{-8}		
Selenium	10	5×10^{-3}	-	1.0×10^{4}	1.0×10^{-4}	-	-
Silver	10	5×10^{-3}	-	6.3×10^{7}	1.59×10^{-8}	-	-
Thallium	2	1×10^{-5}	-	6.7×10^{6}	1.5×10^{-7}	-	-
Tin	-	6×10^{-1}	-	9.2×10^{6}	10.9×10^{-8}	-	-
Titanium	-	-	-	2.3×10^{6}	4.2×10^{-7}	-	-
Zinc	3000	3×10^{-1}	-	1.7×10^{7}	5.9×10^{-8}	$\sim10^{-2}$ to 10^{2}	$\sim10^{-2}$ to 10^{2}
Carbon-based materials							

Diamond	-	-	-	1×10^{-13} to 1×10^{-16}	1×10^{13} to 1×10^{16}	-	-
Graphene	-	-	-	1×10^{8}	1×10^{-8}	-	-
Graphite	-	-	-	2.5×10^{5} to 5.0×10^{6}	2×10^{-5} to 4×10^{-4}	-	-
Metal alloys							
Brass (5% Zn)	-	-	3.34×10^{7}	3.00×10^{-8}	-	-	-
Brass (30% Zn)	-	-	1.67×10^{7}	5.99×10^{-8}	-	-	-
Electrical steel (Non-oriented)	-	-	$\sim4.0\times10^{6}$	$\sim2.5\times10^{-7}$	-	-	-
Low carbon steel	-	-	$\sim6.0\times10^{6}$	$\sim1.7\times10^{-7}$	-	-	-
High carbon steel	-	-	$\sim5.5\times10^{6}$	$\sim1.8\times10^{-7}$	-	-	-
Stainless steel 304	-	-	$\sim1.4\times10^{6}$	$\sim7.1\times10^{-7}$	-	-	-
Stainless steel 316	-	-	$\sim1.3\times10^{6}$	$\sim7.7\times10^{-7}$	-	-	-
Silicon steel	-	-	$\sim4.5\times10^{5}$	$\sim2.2\times10^{-6}$	-	-	-
Tool steel	-	-	$\sim2.5\times10^{6}$ to 7.0×10^{6}	Varies	-	-	-

[a] Italian Legislative Decree n. 152/06

[b] RAIS Risk Assessment Information System https://rais.ornl.gov/index.html

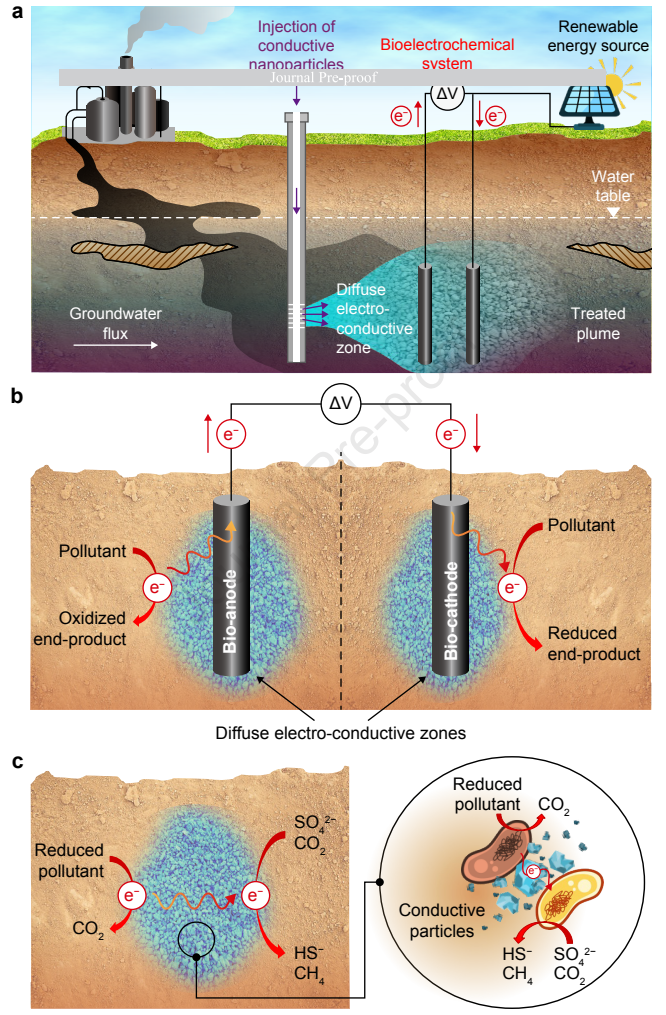
a
Injection of conductive nanoparticles
Bioelectrochemical system
Renewable energy source
Journal Pre-proof
ΔV
e⁻
e⁻
Water table
Diffuse electro-conductive zone
Groundwater flux
Treated plume
b
ΔV
e⁻
e⁻
Pollutant
e⁻
Oxidized end-product
Bio-anode
Bio-cathode
Pollutant
e⁻
Reduced end-product
Diffuse electro-conductive zones
c
Reduced pollutant
e⁻
e⁻
CO2
SO4 2− CO2
HS⁻ CH4
Reduced pollutant
CO2
e⁻
Conductive particles
HS⁻ CH4
SO4 2− CO2

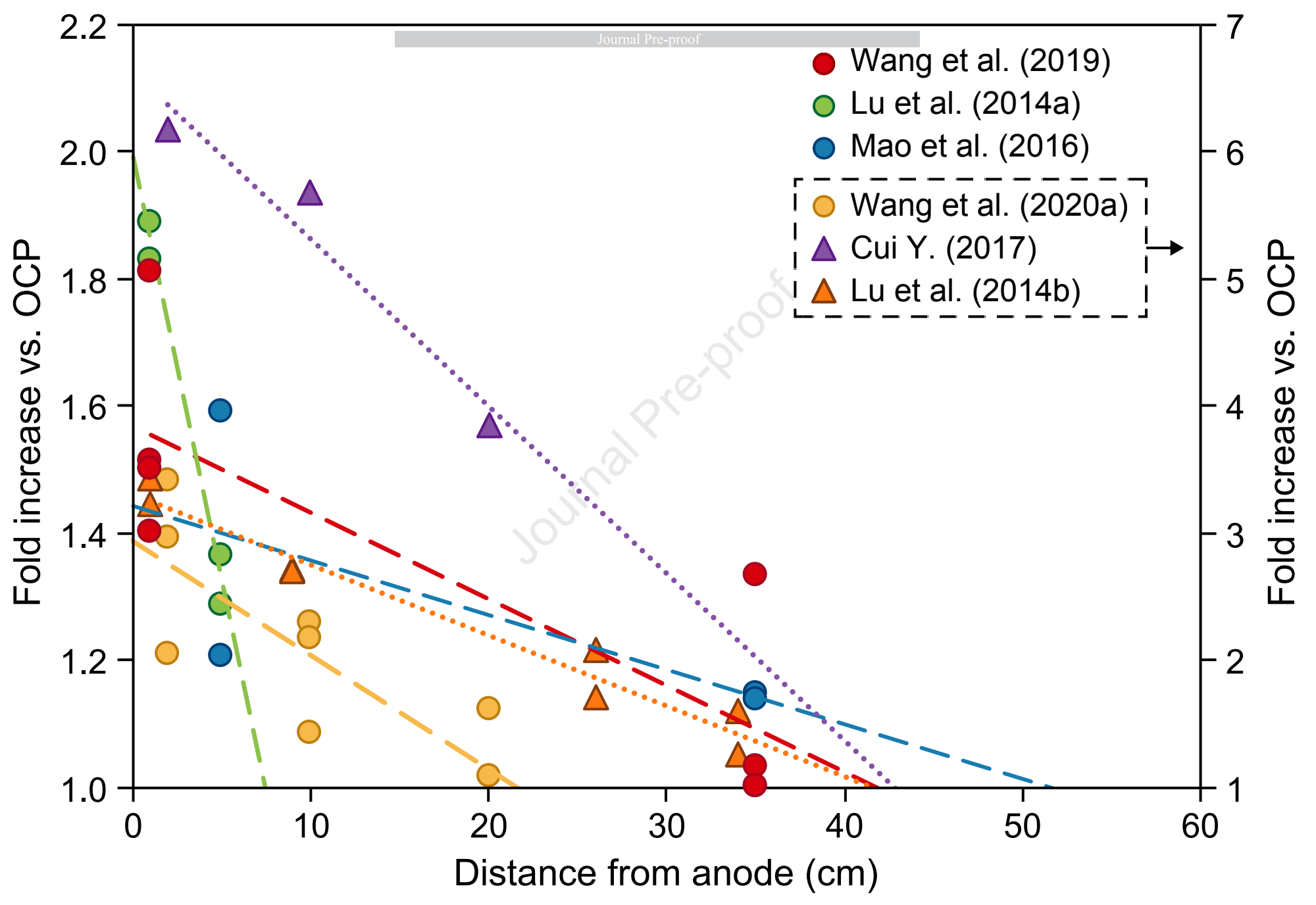
Journal Pre-proof
Wang et al. (2019)
Lu et al. (2014a)
Mao et al. (2016)
Wang et al. (2020a)
Cui Y. (2017)
Lu et al. (2014b)
Fold increase vs. OCP
Fold increase vs. OCP
Distance from anode (cm)
2.2
2.0
1.8
1.6
1.4
1.2
1.0
7
6
5
4
3
2
1
0
10
20
30
40
50
60
Journal Pre-proof

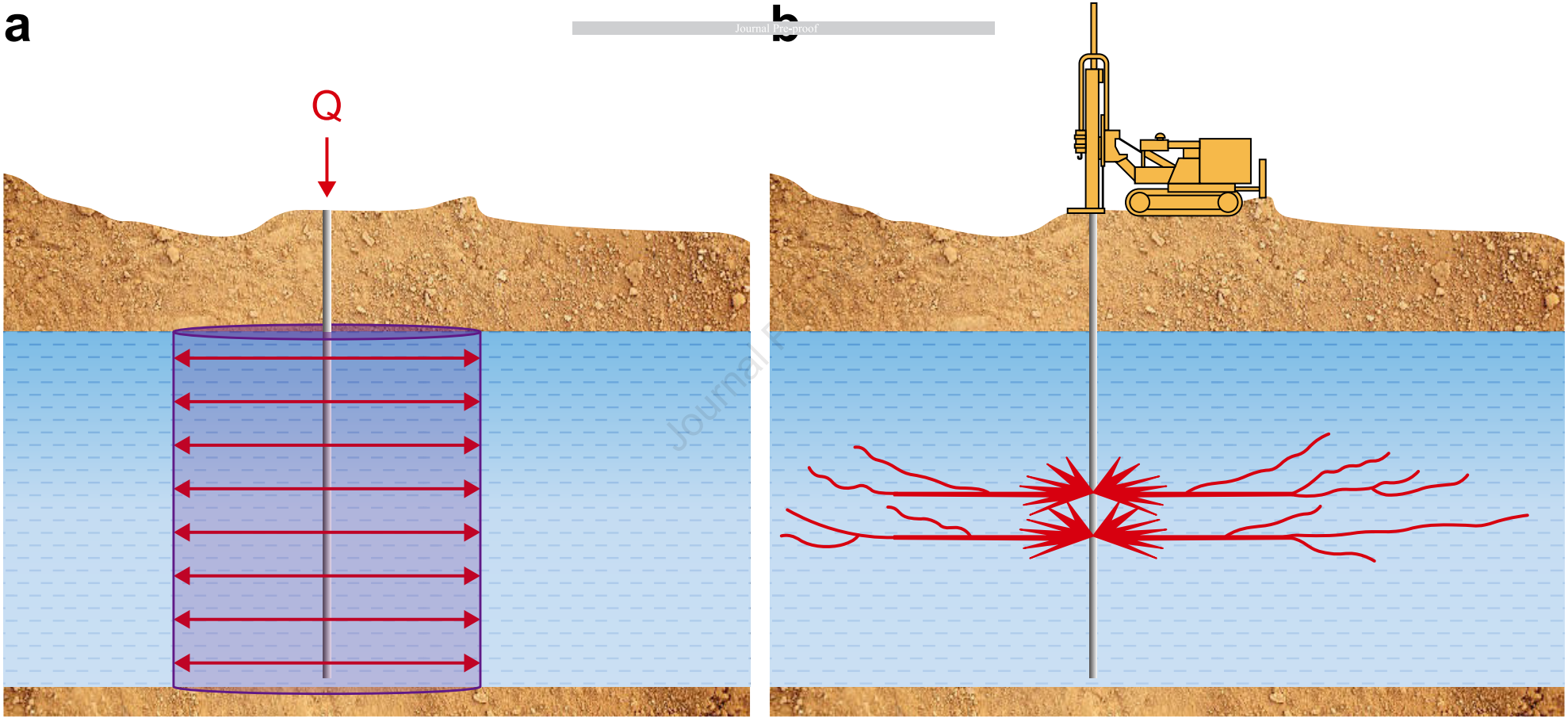

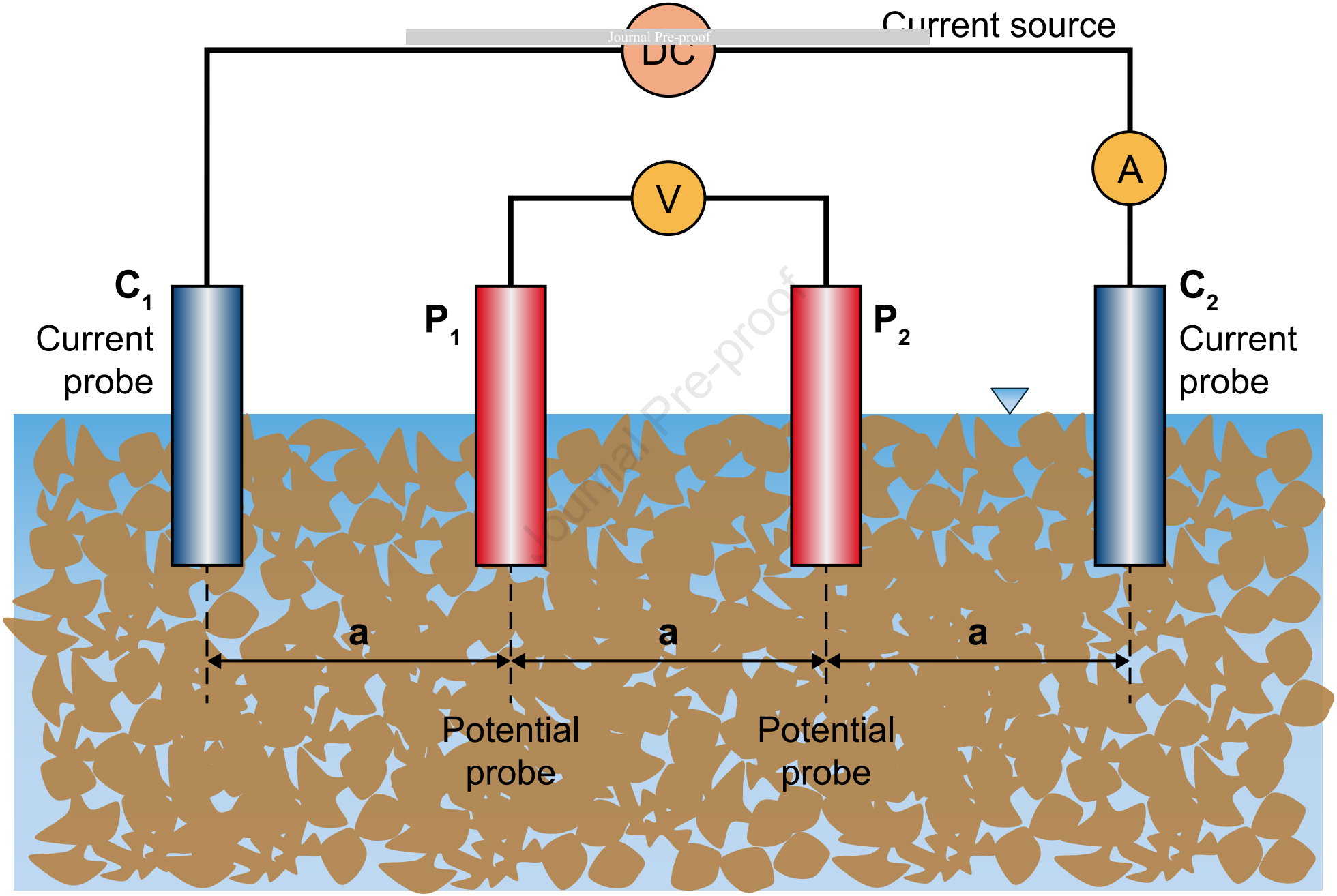

Highlights

1. In situ electro-bioremediation is constrained by the limited radius of influence of traditional electrodes.
2. Subsurface injection of conductive materials enables the formation of diffuse electro-conductive zones (DECZ).
3. DECZ significantly enhance the effectiveness of in situ electro-bioremediation processes.
4. Electrochemical and geophysical techniques provide reliable methods for assessing and sizing DECZ.

Declaration of interests

☒ The authors declare that they have no known competing financial interests or personal relationships that could have appeared to influence the work reported in this paper.

☒ The author is an Editorial Board Member *Environmental Science and Ecotechnology* and was not involved in the editorial review or the decision to publish this article.

☐ The authors declare the following financial interests/personal relationships which may be considered as potential competing interests: